doi:10.1093/brain/awv356 BRAIN 2016: 139; 526–546 | 526

BRAIN
A JOURNAL OF NEUROLOGY

# Metabotropic glutamate receptor 5 couples cellular prion protein to intracellular signalling in Alzheimer's disease

**Laura T. Haas,[1,2] Santiago V. Salazar,[1] Mikhail A. Kostylev,[1] Ji Won Um,[1,*] Adam C. Kaufman[1] and Stephen M. Strittmatter[1]**

**Alzheimer's disease-related phenotypes in mice can be rescued by blockade of either cellular prion protein or metabotropic glutamate receptor 5. We sought genetic and biochemical evidence that these proteins function cooperatively as an obligate complex in the brain. We show that cellular prion protein associates via transmembrane metabotropic glutamate receptor 5 with the intracellular protein mediators Homer1b/c, calcium/calmodulin-dependent protein kinase II, and the Alzheimer's disease risk gene product protein tyrosine kinase 2 beta. Coupling of cellular prion protein to these intracellular proteins is modified by soluble amyloid-β oligomers, by mouse brain Alzheimer's disease transgenes or by human Alzheimer's disease pathology. Amyloid-β oligomer-triggered phosphorylation of intracellular protein mediators and impairment of synaptic plasticity *in vitro* requires *Prnp–Grm5* genetic interaction, being absent in transheterozygous loss-of-function, but present in either single heterozygote. Importantly, genetic coupling between *Prnp* and *Grm5* is also responsible for signalling, for survival and for synapse loss in Alzheimer's disease transgenic model mice. Thus, the interaction between metabotropic glutamate receptor 5 and cellular prion protein has a central role in Alzheimer's disease pathogenesis, and the complex is a potential target for disease-modifying intervention.**

1 Cellular Neuroscience, Neurodegeneration and Repair Program, Department of Neurology, Yale University School of Medicine, New Haven, CT 06536, USA
2 Graduate School of Cellular and Molecular Neuroscience, University of Tuebingen, D-72074 Tuebingen, Germany

*Present address: Department of Physiology and BK21 PLUS Project for Medical Science, Yonsei University College of Medicine, Seoul, Korea

Correspondence to: Stephen M. Strittmatter,
Cellular Neuroscience Neurodegeneration and Repair Program,
BCMM 436, Yale University School of Medicine,
295 Congress Avenue,
New Haven, CT 06536 USA
E-mail: stephen.strittmatter@yale.edu

**Keywords:** Alzheimer's disease; amyloid-beta oligomers; cellular prion protein; metabotropic glutamate receptor 5; homer

**Abbreviations:** APP/PS1$^+$ = amyloid precursor protein/presenilin 1; CamKII = calcium/calmodulin-dependent protein kinase II; eEF2 = eukaryotic elongation factor 2; EPSP = excitatory postsynaptic potential; HEK-293T = human embryonic kidney-293T; Homer1a/b/c = homer scaffolding protein 1 splice variants a/b/c; LTP = long-term potentiation; mGluR5 = metabotropic glutamate receptor 5; $PrP^C$ = cellular prion protein; Pyk2 = proline rich tyrosine kinase 2; RIPA = radioimmunoprecipitation assay

Received June 20, 2015. Revised October 4, 2015. Accepted October 17, 2015. Advance Access publication December 14, 2015

# Introduction

Biomarker studies of late-onset Alzheimer's disease in conjunction with genetic studies of dominantly inherited early-onset cases support the hypothesis that accumulation of amyloid-β peptide triggers the disease. Amongst peptide conformations, soluble oligomers of amyloid-β impair synaptic function and can lead to subsequent tauopathy (Lambert *et al.*, 1998; Kayed *et al.*, 2003; Lesne *et al.*, 2006; Shankar *et al.*, 2008; Jin *et al.*, 2011). An unbiased genome-wide expression cloning experiment identified cellular prion protein ($PrP^C$) as a cell surface binding site for amyloid-β oligomers (Lauren *et al.*, 2009). Amyloid-β oligomers bind to $PrP^C$ with high affinity (Lauren *et al.*, 2009; Balducci *et al.*, 2010; Zou *et al.*, 2011) and multiple studies support a role for $PrP^C$ in mediating Alzheimer's disease-related pathology (Lauren *et al.*, 2009; Chen *et al.*, 2010; Chung *et al.*, 2010; Gimbel *et al.*, 2010; Barry *et al.*, 2011; Bate and Williams, 2011; Freir *et al.*, 2011; Resenberger *et al.*, 2011; Zou *et al.*, 2011; Kudo *et al.*, 2012, 2013; Larson *et al.*, 2012; Um *et al.*, 2012, 2013; Fluharty *et al.*, 2013; Nicoll *et al.*, 2013; Ostapchenko *et al.*, 2013; Rushworth *et al.*, 2013; Dohler *et al.*, 2014; Hu *et al.*, 2014; Klyubin *et al.*, 2014; Walsh *et al.*, 2014). While two studies demonstrated amyloid-β triggered impairment of long-term potentiation (LTP) independently of $PrP^C$ (Calella *et al.*, 2010; Kessels *et al.*, 2010), it has been suggested that different conformations of amyloid-β preparations explain variable outcomes in amyloid-β oligomer toxicity assays (Reed *et al.*, 2011; Nicoll *et al.*, 2013). Critically, the major species of soluble amyloid-β oligomers derived from human Alzheimer's disease brain bind to $PrP^C$ (Um *et al.*, 2012) and require $PrP^C$ to impair LTP *in vivo* (Barry *et al.*, 2011). Among the consequences of amyloid-β oligomers binding to $PrP^C$, downstream activation of FYN kinase alters NMDA (*N*-methyl D-aspartate) receptors and dendritic spine stability (Um *et al.*, 2012). FYN also interacts with tau, such that FYN kinase inhibitors are being examined as agents with disease-modifying action in Alzheimer's disease (Nygaard *et al.*, 2014, 2015; Kaufman *et al.*, 2015).

The altered function and loss of excitatory synapses is a central step in Alzheimer's disease brain dysfunction (Scheff *et al.*, 1990), and $PrP^C$ is essential for synaptic loss induced by amyloid-β oligomers *in vitro* or APP/$PS1^+$ (amyloid precursor protein/presenilin 1) transgene *in vivo* (Gimbel *et al.*, 2010; Um *et al.*, 2012). The metabotropic glutamate receptor 5, mGluR5 (encoded by *GRM5*), is a protein known to provide chronic control over the density and activity of such synapses in a broad range of conditions (Bear *et al.*, 2004). The presence of amyloid-β oligomers alters the trafficking of mGluR5 in neurons, and inhibition of mGluR5 function rescues amyloid-β oligomer or *APP* transgene deficits in synaptic plasticity, synaptic density and memory function *in vivo* (Renner *et al.*, 2010; Um *et al.*, 2013; Hamilton *et al.*, 2014; Hu *et al.*, 2014). mGluR5 is highly accessible to cytosolic binding partners at its large intracellular C-terminal tail, where members of the Homer family of scaffold proteins link mGluR5 to protein kinases and modulate mGluR5 signalling (Brakeman *et al.*, 1997; Xiao *et al.*, 1998; Ango *et al.*, 2001; Mao *et al.*, 2005). One of the kinases associated with both mGluR5 and Homer (encoded by *HOMER1*) is calcium/calmodulin-dependent eukaryotic elongation factor 2 kinase (eEF2K, encoded by *EEF2K*) (Park *et al.*, 2008). eEF2K is released upon activation of mGluR5 to phosphorylate eukaryotic elongation factor 2 (eEF2, encoded by *EEF2*) at T56, a translation elongation controlling protein. Interestingly, amyloid-β oligomer-induced impairment of LTP is dependent on eEF2 phosphorylation at T56 (Ma *et al.*, 2014). Importantly, phosphorylation at this residue is enhanced in the hippocampus of APP/$PS1^+$ Alzheimer's disease model mice as well as in human Alzheimer's disease post-mortem brain samples compared to healthy controls (Ma *et al.*, 2014). eEF2 phosphorylation at T56 inhibits translation of proteins globally (Nairn and Palfrey, 1987), but initiates translation of specific mRNAs, one of which is calcium/calmodulin-dependent protein kinase II (CamKII, encoded by *CAMK2A*) (Scheetz *et al.*, 2000). CamKII has been reported to associate with mGluR5 in a $Ca^{2+}$- and amyloid-β oligomer-dependent manner (Jin *et al.*, 2013*b*; Raka *et al.*, 2015). Analysis of Alzheimer's disease patient brain revealed that autophosphorylated Thr286-CamKII is selectively lost in the frontal cortex and hippocampus of Alzheimer's disease patients compared to age-matched healthy controls (Amada *et al.*, 2005). A further member of the mGluR5 signalling complex is proline-rich tyrosine kinase 2 (Pyk2, encoded by *PTK2B*; also known as protein tyrosine kinase 2 beta or focal adhesion kinase 2) (Nicodemo *et al.*, 2010). A single nucleotide polymorphism in Pyk2 was recently associated with susceptibility to late-onset Alzheimer's disease in a genome-wide association study, emphasizing the potential significance of this kinase for Alzheimer's disease (Lambert *et al.*, 2013; Wang *et al.*, 2015).

While both $PrP^C$ (Lauren *et al.*, 2009; Chen *et al.*, 2010; Chung *et al.*, 2010; Gimbel *et al.*, 2010; Barry *et al.*, 2011; Bate and Williams, 2011; Freir *et al.*, 2011; Resenberger *et al.*, 2011; Zou *et al.*, 2011; Kudo *et al.*, 2012, 2013; Larson *et al.*, 2012; Um *et al.*, 2012, 2013; Fluharty *et al.*, 2013; Nicoll *et al.*, 2013; Ostapchenko *et al.*, 2013; Rushworth *et al.*, 2013; Dohler *et al.*, 2014; Hu *et al.*, 2014; Klyubin *et al.*, 2014; Walsh *et al.*, 2014) and mGluR5 (Um *et al.*, 2013; Hamilton *et al.*, 2014; Hu *et al.*, 2014) are required to mediate Alzheimer's disease-related phenotypes, they may function together in a complex or, alternatively, act independently in Alzheimer's disease pathophysiology. Our previous co-immunoprecipitation experiments suggested a co-dependent mechanism (Um *et al.*, 2013), but extracellular regulation of mGluR5 by endogenous molecules other than glutamate is unique. Importantly, the previous *in vivo* functional tests blocked either mGluR5 or $PrP^C$, and therefore could not

distinguish their independent action from an essential role for amyloid-β oligomer/$PrP^C$ interaction with mGluR5 *in vivo*.

Here we show that coupling between $PrP^C$ and mGluR5 is critically involved in Alzheimer's disease pathology. Our data reveal that $PrP^C$ associates with Homer1b/c, Pyk2, and CamKII selectively when mGluR5 is present. Lowering the gene dosage of both *Prnp* and *Grm5* rescues amyloid-β oligomer-induced deficits in synaptic plasticity *in vitro* and both synapse loss and mouse survival in the APP/$PS1^+$ Alzheimer's disease transgenic model *in vivo*. These data indicate that complex formation between $PrP^C$ and mGluR5 has central significance in Alzheimer's disease. Furthermore, partial blockade of both targets, or their interaction, suggests a promising therapeutic window for modifying the course of Alzheimer's disease.

# Materials and methods

## Amyloid-$\beta_{1\text{-}42}$ preparation

Synthetic amyloid-$\beta_{1\text{-}42}$ peptide was obtained as lyophilized powder from Keck Large Scale Peptide Synthesis Facility (Yale University). Preparation and characterization of amyloid-$\beta_{1\text{-}42}$ monomers and amyloid-$\beta_{1\text{-}42}$ oligomers (amyloid-β oligomers) have been described previously (Um *et al.*, 2012). Amyloid-$\beta_{1\text{-}42}$ fibrils were prepared as amyloid-β oligomers and incubated for 6 months at room temperature. Concentrations of amyloid-β oligomers are expressed in monomer equivalents, with 1 μM total amyloid-$\beta_{1\text{-}42}$ peptide corresponding to ~10 nM oligomeric species (Lauren *et al.*, 2009).

## Mouse strains

Mice were cared for by the Yale Animal Resource Center and all experiments were approved by Yale's institutional animal care and use committee. Mouse strains were maintained on a C57/Bl6J background as described previously (Lu *et al.*, 1997; Jankowsky *et al.*, 2003; Gimbel *et al.*, 2010). Mice were group housed (two to five mice per cage) with a 12-h light/dark cycle.

## Experimental design

All experiments were conducted in a blinded fashion with respect to genotype and treatment. Groups were matched for age and sex. In addition, human brain groups were also matched for post-mortem interval and demographical data. The number of animals used for each subsequent experiment was calculated based on previous experiments to ensure adequate statistical power.

## Preparation of acute mouse brain slices

Mouse brains from 4–12-week-old wild-type, heterozygote or knockout mice were dissected after rapid decapitation. Acute 400-μm coronal slices were cut in ice-cold artificial CSF (119 mM NaCl; 2.5 mM KCl; 1.3 mM $MgSO_4$; 26.2 mM $NaHCO_3$; 11 mM D-glucose; 1.25 mM $NaH_2PO_4$) using a 1000 Plus Vibratome® with steel razor blades. Brain slices were then transferred to brain slice incubators filled with artificial CSF plus 2.4 mM $CaCl_2$ and incubated under constant oxygenation with 95% $O_2$ and 5% $CO_2$. Slices were recovered for 2 h prior to incubation with amyloid-β oligomers for 30 min.

## Crude synaptoneurosome preparation

To purify crude synaptoneurosomes, acute brain slices were homogenized in buffer A [0.32 M sucrose, 20 mM HEPES (pH 7.4), 1 mM EDTA, 1 × PhosSTOP™ and 1 × cOmplete™ Mini protease inhibitor cocktail (Roche)]. Homogenates were centrifuged for 10 min at 875 *g* at 4°C. The supernatant was collected and centrifuged for 10 min at 16 000 *g* at 4°C to obtain a cytosolic fraction (supernatant) and a crude synaptoneurosomal fraction (P2 pellet). P2 pellets were resuspended and sonicated in buffer A prior to use.

## Immunoprecipitation

The protein concentration in crude synaptoneurosomal fractions was determined by Bradford assay (Bio-Rad Protein Assay) prior to immunoprecipation. Crude synaptoneurosomal fractions were pre-cleared from endogenous antibodies for 4 h at 4°C and lysates were incubated overnight with capture antibody (1 μg/ 1 mg of homogenate) at 4°C. The capture antibodies used were Saf32 (Cayman, 189720) and Bar233 (Cayman, 10009036) for anti-$PrP^C$ immunoprecipitation or anti-Myc (Sigma Aldrich, C3956). The preformed antibody-antigen complexes were then incubated with PureProteome™ Protein A/G Mix Magnetic Beads (Millipore, LSKMAGAG10) for 1 h at 4°C under gentle rotation. Beads were washed five times in buffer A prior to elution of proteins in SDS-PAGE (sodium dodecyl sulphate-polyacrylamide gel electrophoresis) sample loading buffer. The immunoprecipitated complexes were then resolved by SDS-PAGE and immunoblotted.

## Immunoblots

Proteins were electrophoresed through precast 4–20% tris-glycine gels (Bio-Rad) and transferred with an iBlot™ Gel Transfer Device (Novex-Life Technologies) onto nitrocellulose membranes (Invitrogen). Loading controls (actin) were run on the same gel. Membranes were blocked (Blocking Buffer for Fluorescent Western Blotting, Rockland MB-070-010) for 1 h at room temperature and incubated overnight in primary antibodies at 4°C. The following primary antibodies were used: anti-actin (Sigma-Aldrich A2066; 1:3000), anti-CaMKII (Abcam ab89197; 1:1000), anti-eEF2 (Cell Signaling Technology #2332; 1:1000), anti-Homer1b/c (Santa Cruz Biotechnology sc-55463; 1:1000), anti-Interleukin-1 beta (R&D systems AB-401-NA; 1:1000), anti-mGluR5/1 (R&D Systems PPS079; 1:1000), anti-phospho-CamKII (Abcam ab5683; 1:1000), anti-phospho-eEF2 (Cell Signalling Technology #2331; 1:1000), anti-phospho-Pyk2 (Cell Signalling #3291; 1:1000), anti-Pyk2 (Cell Signalling #3480; 1:1000) and Saf32 (Cayman 189720; 1:200). Only validated antibodies were used. Validation information can be found on

the company websites or on www.antibodypedia.com. Appropriate secondary antibodies were applied for 1 h at room temperature (Odyssey® donkey anti-mouse or donkey anti-rabbit conjugated to IRDye® 680 or IRDye® 800, LI-COR Biosciences) and proteins were visualized with a LI-COR Odyssey® infrared imaging system. Quantification of band intensities was performed within a linear range of exposure. For co-immunoprecipitates, the level of each precipitated protein is normalized to that protein's input (e.g. Homer co-immunoprecipitate level/Homer input level). This normalized level is further normalized by the normalized PrP level (PrP immunoprecipitate level/PrP input level).

## Cell culture

Human embryonic kidney-293T (HEK-293T) cells were maintained in Dulbecco's modified Eagle medium, supplied with 10% foetal bovine serum, 1% L-glutamine (2 mM final concentration), 1% sodium pyruvate (1 mM final concentration) and 1% penicillin/streptomycin (100 U/ml). Cells were transfected using Lipofectamine® 2000 transfection reagent (Invitrogen). Expression vectors used for rat mGluR5, human $PrP^{C}$, Homer1c, CamKII$\alpha$ and Pyk2 are pcDNA3.1 or pEGFP. HEK-293T cells were harvested 48 h after transfection in buffer A. Cell membranes were prepared using the same protocol as described in the 'Crude synaptoneurosome preparation' section. Here, the P2 pellet was resuspended in radioimmunoprecipitation assay (RIPA) lysis buffer [50 mM Tris-HCl, pH 7.4; 150 mM NaCl; 1% Triton™ X-100; 1 mM EDTA; 0.1% SDS; 0.5% deoxycholic acid; 1 × PhosSTOP™-Roche; 1 × cOmplete™ Mini protease inhibitor cocktail (Roche)] and centrifuged at 100 000 *g* for 1 h at 4°C. The protein concentration in the supernatant was determined by Bradford assay (Bio-Rad Protein Assay) and subjected to immunoprecipitation as described above.

## Mouse brain tissue collection for biochemistry

All mice used for biochemistry were between 12 and 26 months old at the time of analysis with an average age of 644 ± 32 days at the time of sacrifice. Mice were euthanized by rapid decapitation and hippocampus, cortex and cerebellum of brains were rapidly dissected. Brain regions were weighed and homogenized in three times the brain tissue weight in TBS (Tris-buffered saline) containing PhosSTOP™ (Roche) and cOmplete ± Mini protease inhibitor cocktail (Roche) to extract cytosolic proteins. After centrifugation for 30 min at 100 000 *g* and 4°C, the supernatants were collected as TBS-soluble fractions. The remaining pellets were dissolved in three times the original brain tissue weight in RIPA lysis buffer. After centrifugation for 30 min at 100 000 *g* and 4°C, the supernatants were collected as RIPA soluble fractions. The protein concentration in samples was measured by Bradford assay (Bio-Rad Protein Assay) prior to immunoprecipitation or direct separation by SDS-PAGE.

## Human brain tissue collection

Human post-mortem brain tissue was collected as approved by the Institutional Review Board at Yale and stored at −80°C until experimental use. The neuropathological features of Alzheimer's disease in patient's brains were confirmed by classifying them as Braak stage V or higher with a 'frequent' CERAD (Consortium to Establish a Registry for Alzheimer's Disease) neuritic plaque score. Healthy controls were classified as Braak stage 0–II with a CERAD neuritic plaque score of 'none' or 'sparse'. Patient demographic data have been described previously (Kostylev *et al.*, 2015). Parkinson's disease without Alzheimer's features was diagnosed by clinical neuropathological criteria.

Human frontal cortex was homogenized in three times the brain tissue weight in TBS containing PhosSTOP™ (Roche) and cOmplete™ Mini protease inhibitor cocktail (Roche). Homogenates were centrifuged for 30 min at 100 000 *g* and 4°C. The supernatant was again centrifuged for 30 min at 100 000 *g* and 4°C. The supernatant was collected as TBS-soluble fraction. Proteins were extracted from the remaining pellets by centrifugation in three times the original brain tissue weight in TBS + 1% Triton™ X-100 for 30 min at 100 000 *g* and 4°C. The supernatant was collected and again centrifuged for 30 min at 100 000 *g* and 4°C. The protein concentration in the supernatant was measured by Bradford assay (Bio-Rad Protein Assay) and proteins were subjected to immunoprecipitation.

## Analysis of protein activation states after treatment of acute mouse brain slices

Acute mouse brain slices were prepared and treated as described above. Slices were then homogenized in RIPA lysis buffer and centrifuged at 21 000 *g* for 20 min at 4°C. The protein concentration in the RIPA soluble fraction was determined by Bradford assay (Bio-Rad Protein Assay). The RIPA soluble fraction was then mixed with SDS-PAGE sample loading buffer and proteins were resolved by SDS-PAGE followed by immunoblot.

## Electrophysiology

Coronal slices (400 μm) of adult 6–12-week-old mice were prepared as described above and allowed to recover for 1 h prior to recording. Slices were submerged in a recording chamber (BSC-PC, Warner Instruments) containing artificial CSF with 2.4 mM $CaCl_2$ that was continuously oxygenated (95% $O_2$, 5% $CO_2$). Extracellular field recordings were performed in the stratum radiatum of CA1 neurons in the hippocampus by stimulating Schaffer collateral fibres using a bipolar tungsten electrode (TM33CCNON, World Precision Instruments). Extracellular field excitatory postsynaptic potentials (EPSPs) were recorded using a glass microelectrode (2–6 MΩ) (4878, World Precision Instruments) filled with artificial CSF, and placed in the stratum radiatum of CA1 neurons. Test stimuli were induced at 0.033 Hz, and the stimulus intensity was set at 50% of maximal field EPSP slope. A stable baseline was recorded for at least 20 min prior to induction of LTP, and slices were excluded if baseline could not be stabilized after 1 h. LTP was induced by theta burst stimulation (10 bursts of four shocks at 100 Hz, with an interburst interval of 200 ms) given at baseline intensity. Slices were excluded in *post hoc* analysis by pre-established cut-off if 10 or more data points

fell below 75% of baseline level during post-theta burst stimulation recording. Field EPSPs were recorded using an Axon Instruments 700B amplifier and a Digidata 1440 A digitizer, with data analysis performed by pClamp 10 software (Molecular Devices) and Prism 6 software. Amyloid-β oligomers (1 μM), and vehicle were diluted into artificial CSF of the recording chamber and incubated for 30 min prior to LTP induction. Paired-pulse facilitation experiments were performed as described by Kiyota *et al.* (2009) by using a dual pulse at 40-μs duration with stimulus intensity set at 40–60% of maximal field EPSP slope. Pulses were delivered in 20-s intervals and six consecutive responses were averaged for each paired-pulse facilitation test with varying interpulse interval (25, 50, 100, 200, 300 ms). All slices maintained a steady baseline for at least 20 min before paired-pulse facilitation test. The ratio of paired-pulse facilitation was determined by the ratio of the second field EPSP slope divided by the first field EPSP slope in each pair. Input–output responses were recorded from slices that maintained a steady baseline for 20 min. Responses were recorded by increasing stimulus intensity by 0.5 V with 40-μs duration starting at 10–20% of maximal field EPSP.

## Immunohistochemistry of mouse brain slices

All mice used for immunohistochemistry were between 12 and 26 months old at the time of analysis with an average age of 666 ± 35 days at the time of sacrifice. Mice were euthanized and immediately perfused with PBS (phosphate-buffered saline) for 3 min, followed by 4% PFA (paraformaldehyde) for 5 min. Brains were dissected out and fixed in 4% PFA overnight. Brains were sliced into 40 μm parasagittal brain sections using a Leica WT1000S vibratome. Proteins were permeabilized by three washes in PBS + 0.1% Triton™ X-100 for 5 min each. Sections were blocked in 10% normal donkey or normal horse serum (Jackson ImmunoResarch Laboratories) in PBS + 0.1% Triton™ X-100 for 1 h and then incubated with primary antibodies for 16–24 h at 4°C. The following primary antibodies were used: anti-β-amyloid (Cell Signaling Technology 2454; 1:250), anti-GFAP (glial fibrillary acidic protein; Abcam ab7260; 1:500), anti-Iba1 (ionized calcium-binding adapter molecule 1; Wako 019-19741; 1:250), anti-PSD95 (postsynaptic density protein 95; Invitrogen 51-6900; 1:250), and anti-SV2a (synaptic vesicle glycoprotein 2A; Abcam 32942; 1:250). Validation of antibodies is reported on either www.antibodypedia.com or on the company websites. Sections were washed three times in PBS and incubated with secondary antibodies (donkey anti-rabbit or donkey anti-mouse fluorescent antibodies, Invitrogen Alexa Fluor®; 1:500) for 2 h at room temperature. After three washes in PBS, the sections were mounted onto glass slides (SuperFrost™ Plus, Fisher Scientific) and coverslipped with Vectashield (Vector Laboratories H-1200) antifade aqueous mounting medium. Sections used for thioflavin-S (Sigma T1892) staining were mounted onto glass slides (SuperFrost™ Plus, Fisher Scientific), washed in PBS for 5 min and incubated in 0.1% thioflavin-S solution in 70% ethanol at room temperature for 15 min. Slices were washed twice in 70% ethanol and twice in distilled water prior to coverslipping.

## Imaging and analysis of immunohistochemistry

For imaging of synapse density stained by anti-SV2a and anti-PSD95 antibodies, an UltraView Vox spinning disc confocal microscope (PerkinElmer) with a 60 × 1.3 NA oil-immersion lens was used. The area occupied by immunoreactive synaptic puncta from the molecular layer of the dentate gyrus was measured as described previously (Gimbel *et al.*, 2010). For imaging and analysis of the tissue stained for Iba1, GFAP or amyloid-β, a Zeiss AxioImager Z1 fluorescent microscope with a 4 × or 20 × air objective lens was used. The hippocampus, frontal cortex, cortex dorsal to hippocampus and occipital cortex were imaged for each mouse and the area occupied by plaques or cell bodies was analysed by quantification using ImageJ. Statistical analysis was based on separate mice.

## Immunocytochemistry of primary neuronal cultures

Cortical neurons were obtained from embryonic Day 17 wild-type or *Prnp*$^{-/-}$ mouse embryos. After digestion with papain (30 min at 37°C and 5% $CO_2$), the neurons were plated on poly-D-lysine-coated coverslips (BD Biosciences BD354086) placed into 24-well plates or 35 mm cell culture dishes. Neurons were cultured in Neurobasal® A medium supplemented with B-27, 0.5 mM L-glutamate, 1 mM sodium pyruvate, and 1 × penicillin and streptomycin (Invitrogen). At 20–21 days *in vitro*, neurons were treated with 1 μM amyloid-β oligomers or vehicle. Cultures were then fixed in a 4% PFA + 4% sucrose solution, permeabilized with 0.1% Triton™ X-100 in PBS for 15 min and blocked with 10% normal donkey serum for 1 h. Immunostaining of neurons was performed overnight at 4°C. The following primary antibodies were used: anti-Homer (Santa Cruz Biotechnology sc-8921; 1:250), anti-MAP2 (Novus Biologicals NB300-213; 1:2000), anti-mGluR5 (Abcam ab76316; 1:250), anti-phospho-CamKII(T286) (Abcam ab5683; 1:1000), and anti-prion protein (Aves Labs chicken anti-prion protein; 1:1000). www.antibodypedia.com or the company websites offer validation information of all antibodies used in this study. Incubation of neurons with a 1:500 dilution of secondary antibodies (Alexa Fluor® 488, 568 or 633 conjugated donkey anti-rabbit, donkey anti-chicken or donkey anti-goat antibody) was performed for 1 h at room temperature. Coverslips were mounted onto glass slides (SuperFrost™ Plus) with Vectashield (Vector Laboratories H-1200) antifade aqueous mounting medium. Images were acquired on an UltraVIEW Vox spinning disc confocal microscope (PerkinElmer) with a 60 × 1.3 NA oil-immersion lens.

## Measuring the levels of total amyloid-β peptide and $PrP^C$ interacting amyloid-β oligomers

Total amyloid-β levels in TBS-soluble fractions were measured using a commercially available amyloid-$\beta_{1\text{-}42}$ detection kit (Life Technologies KHB3442) and all measurements were performed according to the manufacturer's recommendations. A Victor 3 V plate reader (Perkin Elmer) was used to measure the

absorbance at 450 nm. The absolute amount of amyloid-β was determined using the standard curve based on serial dilutions of a monomeric preparation of synthetic amyloid-β. $PrP^C$-linked immunosorbent assay $PrP^C$-ELISA, which measures $PrP^C$-interacting amyloid-β oligomers, has been described previously (Kostylev *et al.*, 2015).

## Statistics

All results are presented as means ± standard error of the mean (SEM). IBM SPSS Statistics version 21 and Prism 6 software were used for statistical analysis. Data were analysed using one-way or two-way ANOVA, followed by *post hoc* Tukey's multiple comparisons test or Fisher's LSD *post hoc* pairwise comparisons test, as specified in the figure legends. In case of two column comparisons, Mann-Whitney test was used for analysis. Only two-sided tests were used and all data analysed met the assumption for the specific statistical test that was performed. Probability levels of $P < 0.05$ were considered as statistically significant.

# Results

## mGluR5 couples cellular prion protein to intracellular protein mediators

If physiologically relevant brain $PrP^C$/mGluR5 complexes exist, then $PrP^C$ is expected to associate via mGluR5 with a macromolecular assembly that includes multiple intracellular signalling partners. We screened multiple postsynaptic intracellular proteins for association with $PrP^C$ in acute brain slice crude synaptoneurosome preparations (Fig. 1A). Our data show that Homer1b/c, Pyk2, CamKII, and mGluR5 strongly and selectively associate with $PrP^C$ in acute brain slice crude synaptoneurosome preparations (Fig. 1). Genetic deletion of *Grm5* strongly reduced the co-immunoprecipitation signals of intracellular protein mediators in anti-$PrP^C$ immunoprecipitates (Fig. 1B–E). Interestingly, amyloid-β oligomer treatment of acute wild-type brain slices for 30 min dissociated Homer1b/c and Pyk2 from the $PrP^C$ association complex (Fig. 1B–D). Notably, amyloid-β oligomer stimulation enhanced the association between $PrP^C$ and CamKII as well as between $PrP^C$ and mGluR5 (Fig. 1B, E and F). Our data further show that association changes between the $PrP^C$-mGluR5 complex and intracellular protein mediators is specifically triggered by the oligomeric form of amyloid-β, but not monomeric amyloid-β or amyloid-β fibrils (Supplementary Fig. 1A–D).

We also examined the acute amyloid-β oligomer-induced dissociation of Homer from the receptor complex histologically (Supplementary Fig. 2). The co-localization of mGluR5 and Homer was extensive in cortical neurons with a punctate dendritic pattern, which largely overlapped with $PrP^C$ distribution. Exposure to amyloid-β oligomers significantly reduced Homer co-localization with mGluR5 in wild-type, but not in *Prnp* null neurons (Supplementary Fig. 2). Thus, the proximity of Homer, mGluR5 and $PrP^C$ is disrupted by amyloid-β oligomers in a $PrP^C$-dependent manner in neurons.

The synaptic structures in brain slices contain many components, therefore we sought to determine if the marked reduction of co-immunoprecipitation between $PrP^C$ and intracellular mediators in $Grm5^{-/-}$ slices implies direct coupling of these molecules through mGluR5. We examined a simplified non-neuronal HEK-293T cell system expressing only the neuronal proteins in question to assess whether mGluR5 is not only necessary but also sufficient for complex formation between $PrP^C$ and intracellular signalling proteins. Cells co-expressing $PrP^C$, Homer1c, Pyk2 and CamKIIα revealed minimal co-immunoprecipitation signals of Homer1c, Pyk2 and CamKIIα in anti-$PrP^C$ immunoprecipitates. This signal was strongly enhanced by co-expressing either Myc-mGluR5 or Myc-mGluR1 (Fig. 2A–D). We sought to recapitulate the amyloid-β oligomer-induced association changes in anti-$PrP^C$ immunoprecipitates we observed in acute mouse brain slices. Amyloid-β oligomer stimulation of HEK-293T cells co-expressing $PrP^C$, Myc-mGluR5, Homer1c, Pyk2 and CamKIIα significantly reduced Homer1c and Pyk2 signals in anti-$PrP^C$ immunoprecipitates, similar to what we observed in acute brain slice crude synaptoneurosome preparations (Fig. 2A–C). In contrast, amyloid-β oligomer treatment enhanced the co-immunoprecipitation signal of CamKIIα in anti-$PrP^C$ immunoprecipitates (Fig. 2A and D). Amyloid-β oligomers failed to modulate the interaction between $PrP^C$ and Homer1c, Pyk2 or CamKIIα when Myc-mGluR1 was expressed instead of Myc-mGluR5, consistent with a selective role of mGluR5 related to Alzheimer's disease (Fig. 2A–D). Notably, treatment of cells with amyloid-β oligomers for 30 min enhanced the association between $PrP^C$ and Myc-mGluR5 but not between $PrP^C$ and the closely related Myc-mGluR1 (Fig. 2A and E). We found similar results in the complementary anti-Myc immunoprecipitation. Amyloid-β oligomers were unable to modulate the interaction between Myc-mGluR5 and Homer1c, Pyk2 or CamKIIα in HEK-293T cells in the absence of $PrP^C$ (Fig. 2A and F–H). Moreover, amyloid-β oligomers were only able to selectively modulate the interaction between Myc-mGluR and Homer1c, Pyk2 or CamKIIα in cells co-expressing $PrP^C$ and Myc-mGluR5, but not $PrP^C$ and Myc-mGluR1 (Fig. 2A and F–H). Thus, mGluR5 links $PrP^C$ with a class of intracellular signalling proteins in an amyloid-β oligomer-regulated manner.

Having observed amyloid-β oligomer regulation of the physical association of $PrP^C$ with intracellular signalling proteins via mGluR5 *in vitro*, we assessed this phenomenon in the brain. For brain lysates from aged APP/PS1$^+$ mouse model hippocampus with Alzheimer's disease pathology, anti-$PrP^C$ immunoprecipitates showed significantly reduced Pyk2 and Homer1b/c signals compared to wild-type (Fig. 3A, D and F). Based on these positive findings from the mouse model, we examined evidence for altered

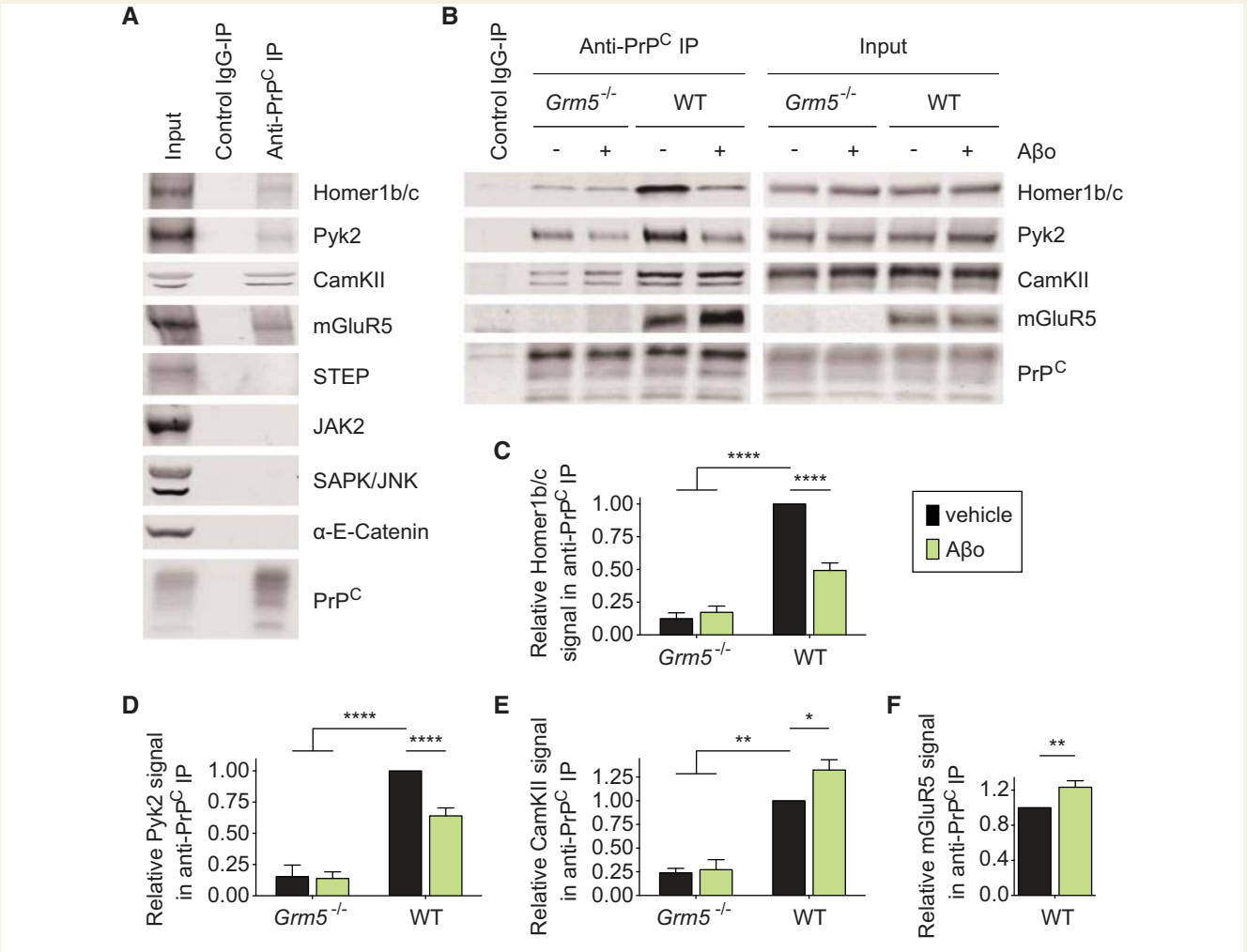


**Figure 1 mGluR5 couples PrP$^C$ to intracellular protein mediators in acute mouse brain slices.** (**A**) Representative immunoblots showing co-immunoprecipitation (co-IP) between PrP$^C$ and Homer1b/c, Pyk2, CamKII and mGluR5 in acute mouse brain slice crude synaptoneurosome preparations. In contrast, STEP, JAK2, SAPK/JUNK and α-E-catenin are not precipitated. (**B**) Co-immunoprecipitation between PrP$^C$ and Homer1b/c, Pyk2 and CamKII is largely reduced by genetic deletion of *Grm5* and altered by acute amyloid-β oligomer treatment. Genotype and treatment of acute brain slices is indicated above each lane. (**C–F**) Densitometric analysis of the immunoblots from **B**, analysed by one-way ANOVA with *post hoc* Tukey's multiple comparisons test (**C–E**) and by Mann-Whitney test (**F**). Data are mean ± SEM, $n = 14$ wild-type mice and $n = 3$ *Grm5*$^{-/-}$ mice. (**C**) Co-immunoprecipitation between PrP$^C$ and Homer1b/c is significantly reduced in *Grm5*$^{-/-}$ acute brain slice crude synaptoneurosome preparations and in wild-type acute brain slice crude synaptoneurosome preparations after amyloid-β oligomer treatment (****$P < 0.0001$). (**D**) Co-immunoprecipitation between PrP$^C$ and Pyk2 is significantly reduced in acute *Grm5*$^{-/-}$ brain slice crude synaptoneurosome preparations and in acute wild-type brain slice crude synaptoneurosome preparations after amyloid-β oligomer treatment (****$P < 0.0001$). (**E**) Co-immunoprecipitation between PrP$^C$ and CamKII is significantly reduced in *Grm5*$^{-/-}$ acute brain slice crude synaptoneurosome preparations (**$P < 0.01$), but enhanced in wild-type acute brain slice crude synaptoneurosome preparations after amyloid-β oligomer treatment (*$P < 0.05$). **F.** Treatment of acute brain slices with 1 μM amyloid-β oligomers for 30 min significantly enhanced the mGluR5 signal in anti-PrP$^C$ immunoprecipitates (*$P < 0.05$). Aβo = amyloid-β oligomer; WT = wild-type.

coupling of PrP$^C$ with Homer1b/c and Pyk2 in human autopsy brain samples. We observed a similar reduction of Pyk2 and Homer1b/c signals in anti-PrP$^C$ immunoprecipitates from Alzheimer's disease post-mortem frontal cortex compared to tissue from age-matched neurologically healthy controls or Parkinson's disease subjects (Fig. 3B, G and H). Thus, the physical association of mGluR5-dependent signalling molecules with PrP$^C$ is regulated by amyloid-β pathology in mouse and human disease.

## Genetic coupling between *Prnp* and *Grm5* mediates acute alterations in protein activation states

Our study revealed that mGluR5 connects amyloid-β oligomer-PrP$^C$ to intracellular protein mediators. We sought to determine if there is a genetic interaction between *Prnp* and *Grm5* with regard to amyloid-β oligomer-induced signalling within neurons. Previous studies proposed an

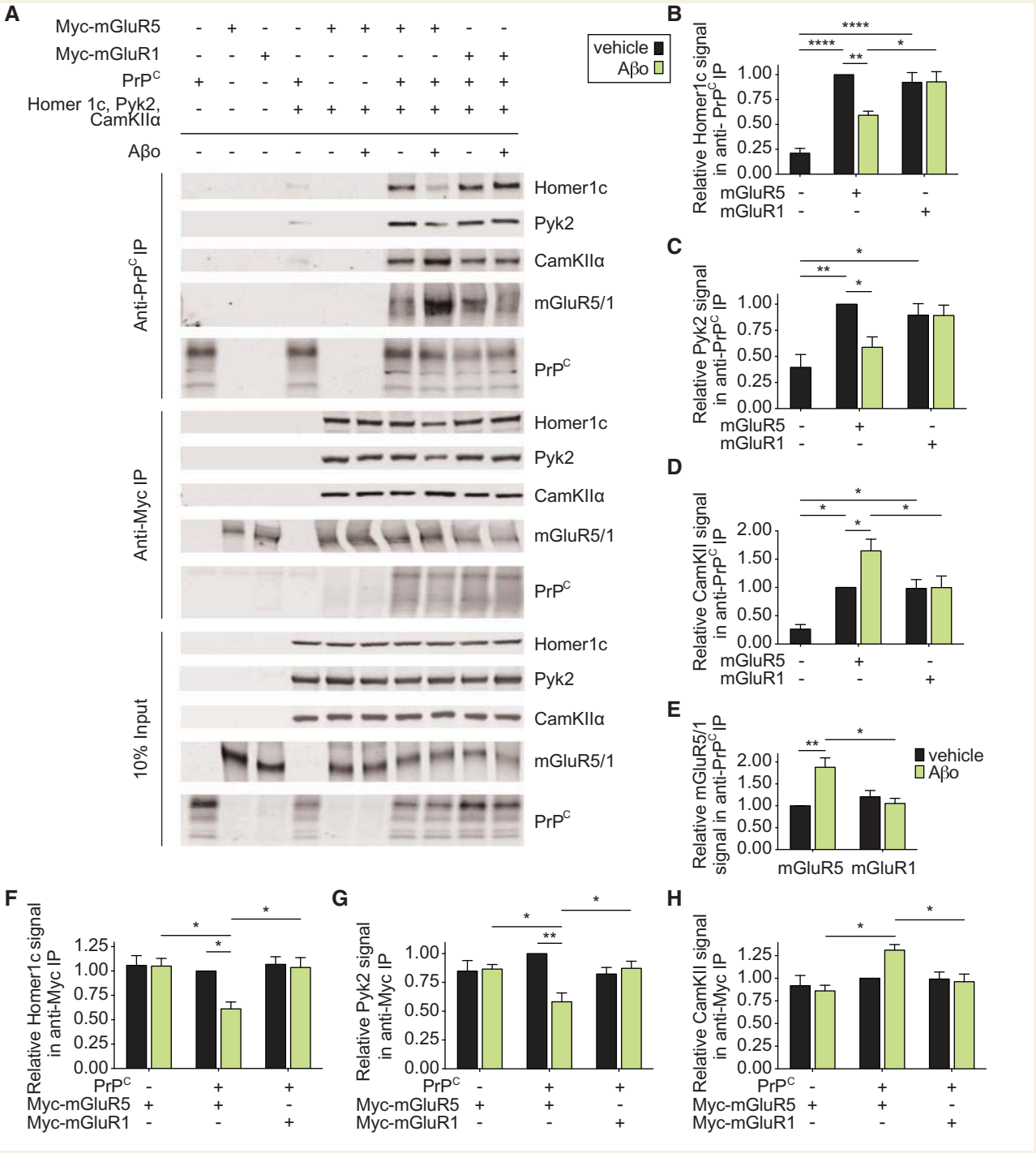


**Figure 2 mGluR5 couples PrP$^C$ to intracellular protein mediators in HEK-293T cells.** (**A**) Representative immunoblots of co-immunoprecipitation between PrP$^C$ and Myc-mGluR5, Homer1c, Pyk2, and CamKII$\alpha$ or between Myc-mGluR and PrP$^C$, Homer1c, Pyk2, and CamKII$\alpha$ in HEK-293T cells. Transfection of plasmids and treatment with 1 $\mu$M amyloid-$\beta$ oligomers for 30 min is indicated above each lane. The input panel displays proteins in 10% input of the anti-Myc immunoprecipitation experiment. The 10% input of the anti-PrP$^C$ experiment depicted comparable protein expression and is not replicated here. (**B–H**) Densitometric analysis of the immunoblots from **A**, analysed by one-way ANOVA with *post hoc* Tukey's multiple comparisons test. Data are mean $\pm$ SEM, $n = 5$ for anti-PrP$^C$ immunoprecipitation and $n = 4$ for anti-Myc immunoprecipitation. (**B–D**) Co-immunoprecipitation between PrP$^C$ and Homer1c (**B**), Pyk2 (**C**) and CamKII$\alpha$ (**D**) is significantly enhanced by co-expression of either Myc-mGluR5 or Myc-mGluR1. Amyloid-$\beta$ oligomer treatment significantly modulates co-immunoprecipitation in Myc-mGluR5- but not Myc-mGluR1-coexpressing cells (****$P < 0.0001$; **$P < 0.01$; *$P < 0.05$). (**E**) Amyloid-$\beta$ oligomer treatment of HEK-293T cells overexpressing PrP$^C$ and Myc-mGluR5 but not PrP$^C$ and Myc-mGluR1 significantly enhances the Myc-mGluR5 signal in anti-PrP$^C$ immunoprecipitates (**$P < 0.01$; *$P < 0.05$). (**F–H**) Co-immunoprecipitation between Myc-mGluR and Homer1c (**F**), Pyk2 (**G**) and CamKII$\alpha$ (**H**). Amyloid-$\beta$ oligomer-treatment of HEK-293T cells co-expressing PrP$^C$ and Myc-mGluR5 but not Myc-mGluR1 significantly alters co-immunoprecipitation signals (**$P < 0.01$; *$P < 0.05$). Aβo = amyloid-$\beta$ oligomer; WT = wild-type.

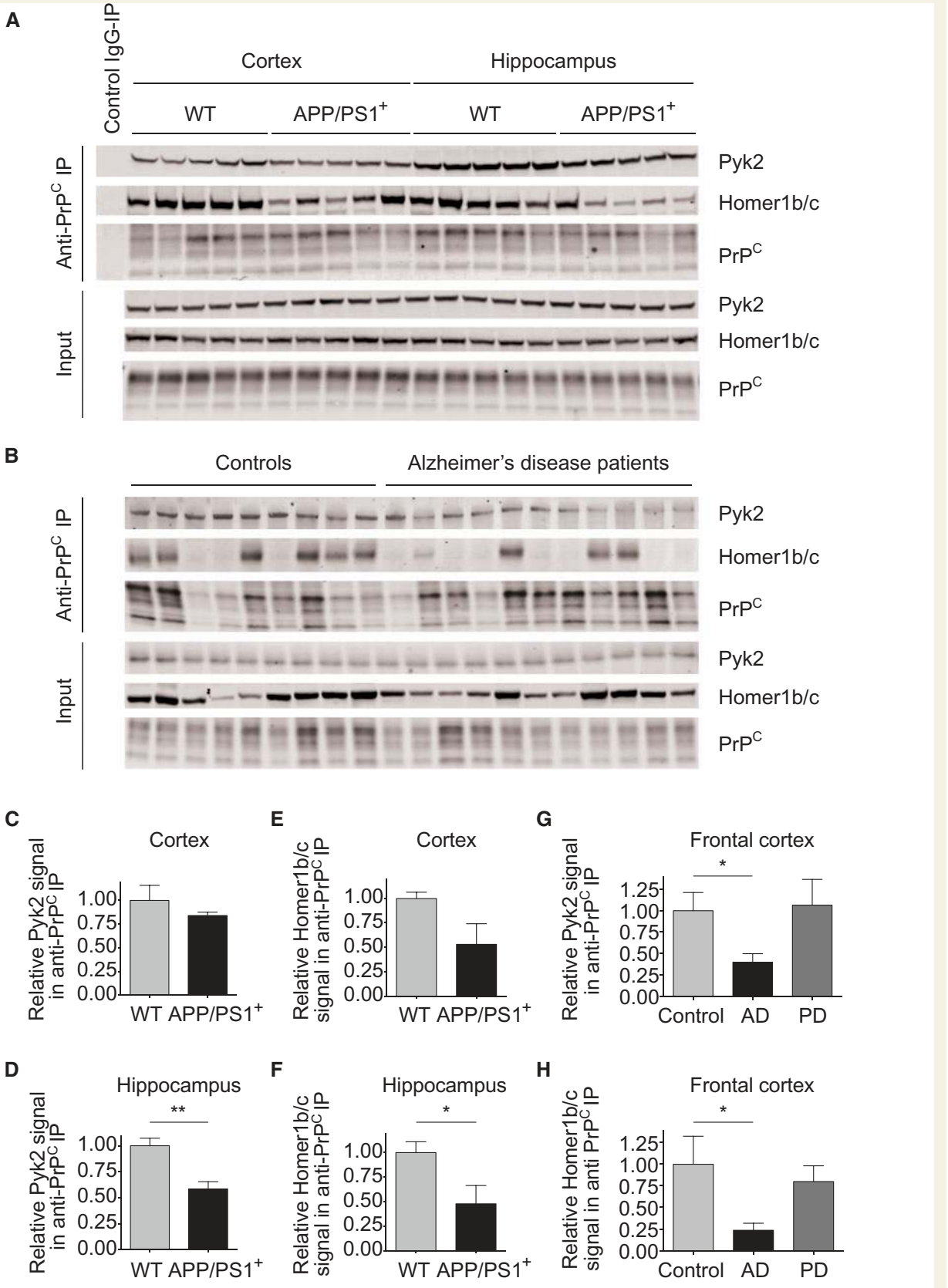


**Figure 3 The coupling between $PrP^C$ and intracellular protein mediators is pathologically altered in Alzheimer's model mice and in human Alzheimer's disease patients.** (**A**) Representative immunoblots of brain region-specific lysates of age-matched 14–19-month-old wild-type and APP/PS1$^+$ brain. (**B**) Representative immunoblots of human frontal cortex of 50–90-year-old controls ($n$ = 9) and 52–89-year-old Alzheimer's disease patients ($n$ = 11). (**C–F**) Densitometric analysis of the immunoblots from **A**. Data are mean ± SEM, $n$ = 5

(continued)

important role of alterations in protein phosphorylation states in contributing to Alzheimer's disease pathogenesis. We analysed whether amyloid-β oligomer stimulation of acute brain slices activates the specific mGluR5 signalling proteins found to be associated with $PrP^C$. Thirty minutes amyloid-β oligomer stimulation of acute brain slices significantly increased phospho-Pyk2(Y402) and phospho-CamKII(T286) levels (Fig. 4). We verified that activation of Pyk2 and CamKII is mediated by the oligomeric form of amyloid-β only, but not monomeric amyloid-β or amyloid-β fibrils (Supplementary Fig. 1F–H). We found that amyloid-β oligomer-induced activation of Pyk2(Y402) and CamKII(T286) was not significantly altered by removal of one allele of either *Prnp* or *Grm5* (Fig. 4). However, removal of one allele of both *Prnp* and *Grm5* significantly reduced amyloid-β oligomer-induced phosphorylation changes (green bars compared to black bars; Fig. 4). Moreover, amyloid-β oligomer treatment failed to activate Pyk2 at Y402 and CamKII at T286 in $Prnp^{-/-}$ as well as in $Grm5^{-/-}$ acute brain slices (yellow and blue bars; Fig. 4). A two-way ANOVA with *post hoc* Tukey's multiple comparisons test for *Prnp* and *Grm5* was performed to verify a significant interaction between *Prnp* and *Grm5* in triggering amyloid-β oligomer-induced aberrant phosphorylation states (Fig. 4). Notably, the deletion of a single *Prnp* or *Grm5* allele does not influence the reciprocal protein expression in heterozygote mouse brain (Supplementary Fig. 3). Thus, the synthetic phenotype for amyloid-β oligomer signalling in the trans-heterozgous state demonstrates genetic interaction between $PrP^C$ and mGluR5 in Alzheimer's disease-related signal transduction biochemistry.

## Genetic coupling between *Prnp* and *Grm5* mediates acute amyloid-β oligomer-induced impairment of synaptic plasticity

To provide further genetic evidence for the coupling between $PrP^C$ and mGluR5 in amyloid-β oligomer signalling, we investigated the effect of amyloid-β oligomers on LTP in the Schaffer collateral pathway between CA3 and CA1 neurons in acute brain slices. We found that amyloid-β oligomers significantly reduce the slope of the field EPSP in wild-type (Fig. 5A), $Prnp^{+/-}$ (Fig. 5B) and $Grm5^{+/-}$ (Fig. 5C) brain slices following theta burst stimulation. However, amyloid-β oligomers failed to inhibit LTP in $Prnp^{+/-}$ $Grm5^{+/-}$ brain slices (Fig. 5D). Comparing across genotypes without amyloid-β oligomer pretreatment, the extent of LTP was indistinguishable (Fig. 5E). In the presence of amyloid-β oligomers, removal of one allele of either *Prnp* or *Grm5* did not significantly alter the magnitude of LTP (Fig. 5F). In contrast, deletion of one allele for both *Prnp* and *Grm5* was able to significantly rescue amyloid-β oligomer-dependent inhibition of LTP seen in wild-type slices (Fig. 5F). A two-way ANOVA for *Prnp* and *Grm5* confirmed a significant interaction between both genes in mediating amyloid-β oligomer-dependent deficits in LTP (Fig. 5G). We considered whether the lack of amyloid-β oligomer responsiveness in the double heterozygote state as due to altered baseline excitatory neurotransmission. We performed paired-pulse experiments at varying lengths to determine whether glutamate release probability was affected by *Prnp or Grm5* heterozygosity (Supplementary Fig. 4A). Paired-pulse ratios approached 1.0 with increasing interval length, and did not vary significantly with respect to genotype. These results suggest glutamate signalling remains unchanged in single and double heterozygote *Prnp* and/or *Grm5* brain slices. Furthermore, we measured input-output curves to determine baseline synaptic transmission in all genotypes. We recorded field EPSPs in the CA1 of the hippocampus of wild-type, $Prnp^{+/-}$, $Grm5^{+/-}$, and $Prnp^{+/-}$ $Grm5^{+/-}$ brain slices. Baseline synaptic transmission remained unchanged across genotypes (Supplementary Fig. 4B). Together these data demonstrate a genetic interaction between $PrP^C$ and mGluR5 in mediating acute amyloid-β oligomer-induced biochemical signalling and electrophysiological plasticity.

## Genetic coupling between *Prnp* and *Grm5* mediates alterations in protein activation states in Alzheimer's mice

The preceding data show that mGluR5 physically and genetically couples $PrP^C$ to intracellular signalling proteins during acute exposure to amyloid-β oligomers. Next, we analysed the genetic coupling in a chronic Alzheimer's disease model, $APP/PS1^+$ transgenic mice. We have shown previously that acute amyloid-β oligomer treatment and TBS-soluble extracts from human Alzheimer's disease patients, but not controls, trigger phosphorylation of eEF2 at

**Figure 3** Continued

mice. (**C**) Co-immunoprecipitation between $PrP^C$ and Pyk2 in cortical lysates. (**D**) The Pyk2 signal in anti-$PrP^C$ immunoprecipitates is significantly reduced in $APP/PS1^+$ hippocampus compared to wild-type (**$P < 0.01$) by Mann-Whitney test. (**E**) Co-immunoprecipitation between $PrP^C$ and Homer1b/c in cortical lysates. (**F**) The Homer1b/c signal in anti-$PrP^C$ immunoprecipitates is significantly reduced in $APP/PS1^+$ hippocampus compared to wild-type (*$P < 0.05$) by unpaired *t*-test with Welch's correction. (**G–H**) Densitometric analysis of the immunoblots from **B**, analysed by Mann-Whitney test. Data are mean ± SEM. The Pyk2 (**G**) and Homer1b/c (**H**) signal in anti-$PrP^C$ immunoprecipitates is significantly reduced in Alzheimer's disease (AD) frontal cortex compared to controls (*$P < 0.05$). Pyk2 and Homer1b/c levels in anti-$PrP^C$ immunoprecipitates of 59–86-year-old Parkinson's disease (PD) patients ($n = 3$) are not significantly different to controls.

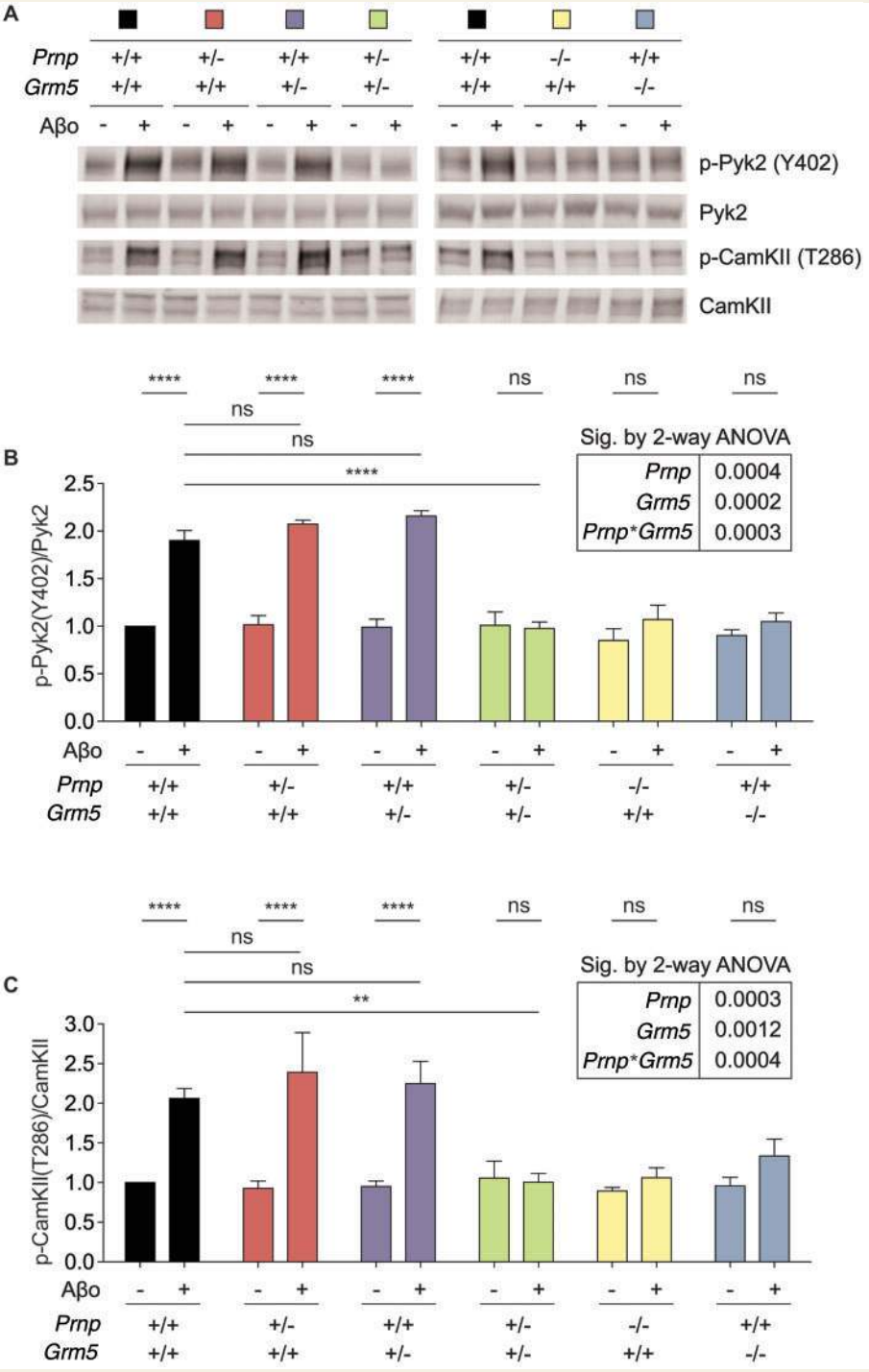


**Figure 4 Genetic coupling between *Prnp* and *Grm5* mediates alterations in protein activation states in acute brain slices.** (**A**) Representative immunoblots showing enhanced Pyk2(Y402) and CamKII(T286) phosphorylation after amyloid-β oligomer treatment in acute wild-type and single heterozygote brain slices, but not in double heterozygote or single knockout brain slices. Genotype and treatment with 1 μM amyloid-β oligomers for 30 min is indicated above each lane. (**B** and **C**) Densitometric analysis of the immunoblots from **A**, analysed by one-way and two-way ANOVA with Tukey's multiple comparisons test. Data are mean ± SEM, $n = 13$ wild-type mice and $n = 3$ for every other genotype. Amyloid-β oligomer treatment increases phosphorylation of Pyk2 at Y402 (**B**) and CamKII at T286 (**C**) in wild-type and single heterozygote brain slices (****$P < 0.0001$), but not in double heterozygote or single knockout slices ($P > 0.05$). Amyloid-β oligomer-induced enhanced phosphorylation is not significantly different between wild-type and single heterozygote brain slices ($P > 0.05$). Removal of one allele of both *Grm5* and *Prnp* significantly reduces amyloid-β oligomer-induced enhanced Pyk2(Y402)-phosphorylation (****$P < 0.0001$) and CamKII(T286)-phosphorylation (**$P < 0.01$). A two-way ANOVA with *post hoc* Tukey's multiple comparisons test for *Prnp* and *Grm5* showed a significant interaction between *Prnp* and *Grm5* in triggering amyloid-β oligomer-induced enhanced phosphorylation of Pyk2 ($P = 0.0003$) and CamKII ($P = 0.0004$). Aβo = amyloid-β oligomer; ns = not significant.

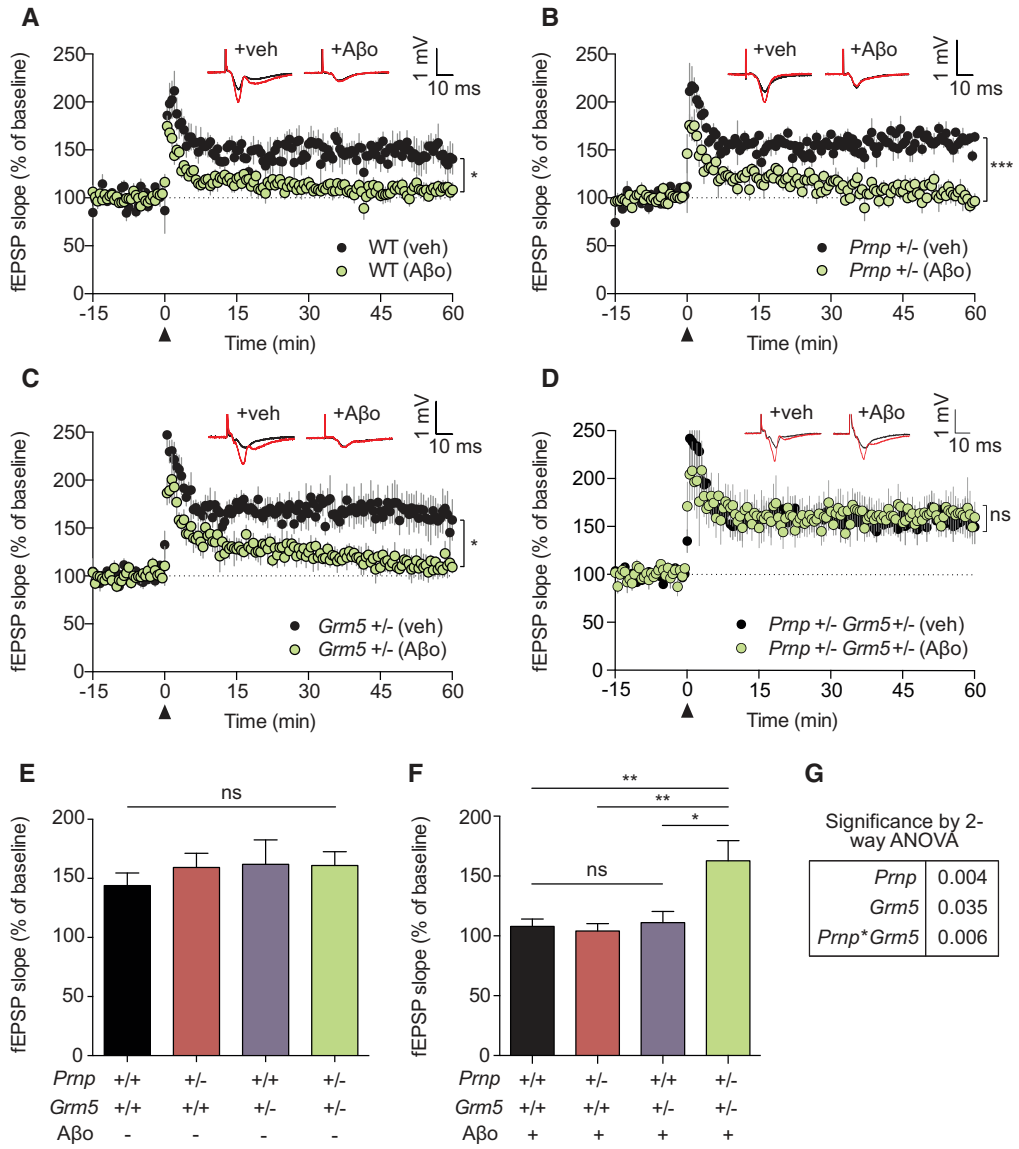


**Figure 5 Genetic coupling between *Prnp* and *Grm5* mediates acute amyloid-β oligomer-induced impairment of synaptic plasticity.** Field potentials were recorded from the CA1 region of adult wild-type (**A**), *Prnp*$^{+/-}$ (**B**), *Grm5*$^{+/-}$ (**C**), and *Prnp*$^{+/-}$ *Grm5*$^{+/-}$ (**D**) brain slices. The slope of the field EPSP (fEPSP)is plotted as a function of time. Representative traces immediately before theta burst stimulation (denoted by arrowhead at 0 min; black) and 60 min post- theta burst stimulation (red) are superimposed (average six sweeps) in each respective graph. Data are graphed as mean ± SEM of averaged slices per animal. Slices were treated with either vehicle (wild-type: five mice, six slices; *Prnp*$^{+/-}$: four mice, seven slices; *Grm5*$^{+/-}$: six mice, seven slices; *Prnp*$^{+/-}$ *Grm5*$^{+/-}$: six mice, 11 slices) or 1 μM amyloid-β oligomers (wild-type: seven mice, 12 slices; *Prnp*$^{+/-}$: six mice, eight slices; *Grm5*$^{+/-}$: five mice, six slices; *Prnp*$^{+/-}$ *Grm5*$^{+/-}$: five mice, five slices) 30 min prior to theta burst stimulation. Field EPSPs in 50–60 min post-theta burst stimulation are significantly decreased in amyloid-β oligomer-treated slices compared to vehicle treated for wild-type, *Prnp*$^{+/-}$ and *Grm5*$^{+/-}$ (*$P < 0.05$; ***$P < 0.001$), but not *Prnp*$^{+/-}$ *Grm5*$^{+/-}$ slices by two-tailed *t*-test. (**E** and **F**) Field EPSPs are graphed as mean ± SEM of all slices per genotype (**E**). Field EPSPs in the 50–60-min post-theta burst stimulation are not different between vehicle-treated slices. (**F**) Field EPSPs in amyloid-β oligomer-treated *Prnp*$^{+/-}$ *Grm5*$^{+/-}$ slices are significantly enhanced when analysed by one-way ANOVA with *post hoc* Tukey's multiple comparisons test (**$P < 0.01$; *$P < 0.05$). (**G**) A two-way ANOVA with *post hoc* Tukey's multiple comparisons test for *Prnp* and *Grm5* showed a significant interaction between *Prnp* and *Grm5* in triggering amyloid-β oligomer-induced inhibition of LTP. Aβo = amyloid-β oligomer; WT = wild-type.

T56 in cortical neurons (Um *et al.*, 2013). Here we found that phospho-Pyk2(Y402) and phospho-eEF2(T56) levels were significantly enhanced in APP/PS1$^{+}$ hippocampus (black bar compared to grey bar; Fig. 6A, B and D). Enhanced phospho-Pyk2(Y402) and phospho-eEF2(T56) levels were not significantly altered by removal of one allele of either *Prnp* or *Grm5* (black bar compared to red and purple bar; Fig. 6A, B and D). Pyk2(Y402) and

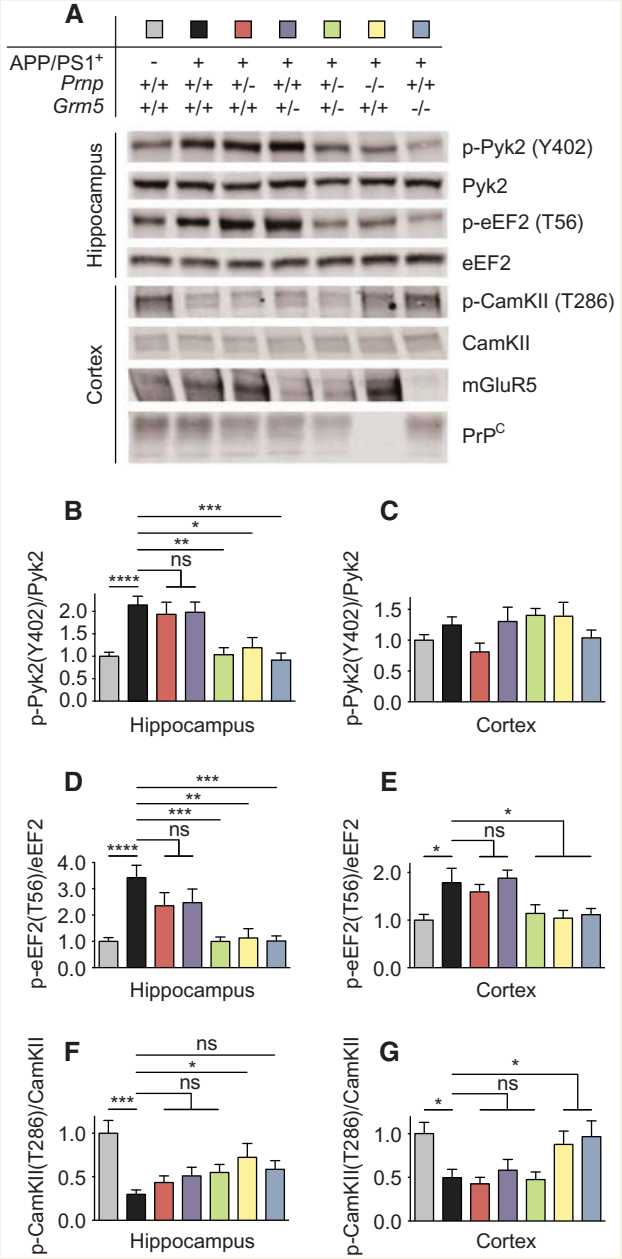


**Figure 6 Genetic coupling between *Prnp* and *Grm5* mediates chronic alterations in protein activation states in Alzheimer's model mice *in vivo*.** **(A)** Representative immunoblots of brain region-specific lysates revealed altered Pyk2(Y402), eEF2(T56) and CamKII(T286) phosphorylation in APP/PS1$^+$ brain compared to wild-type brain, which is recovered in APP/PS1$^+$ *Prnp*$^{+/-}$ *Grm5*$^{+/-}$, APP/PS1$^+$ *Prnp*$^{-/-}$ and APP/PS1$^+$ *Grm5*$^{-/-}$ brain at an average age of 644 ± 32 days. Samples derive from one experiment and all gels/blots were processed in parallel. A sample processing control was included on all gels. (**B–G**) Densitometric analysis of the immunoblots from **A**, analysed by one-way ANOVA with *post hoc* Tukey's multiple comparisons test, unless otherwise stated. Mean ± SEM, $n = 12$ mice (wild-type and APP/PS1$^+$), $n = 6$ mice (every other genotype). (**B**) Phospho-Pyk2(Y402) levels are enhanced in APP/PS1$^+$ hippocampus (****$P < 0.0001$), which is not different to APP/PS1$^+$ single het erozygous hippocampus. Enhanced phospho-Pyk2(Y402) levels are reduced in APP/PS1$^+$ *Prnp*$^{+/-}$ *Grm5*$^{+/-}$, APP/PS1$^+$ *Prnp*$^{-/-}$ and APP/PS1$^+$ *Grm5*$^{-/-}$ hippocampus eEF2(T56) phosphorylation in APP/PS1$^+$ hippocampus was significantly reduced by lowering the gene dosage of both *Prnp* and *Grm5* as well as by full genetic deletion of either *Prnp* or *Grm5* (green, yellow and blue bar compared to black bar; Fig. 6A, B and D). While Pyk2 phosphorylation at Y402 was unaltered between wild-type and APP/PS1$^+$ mouse cortex (Fig. 6C and Supplementary Fig. 5A), eEF2 phosphorylation at T56 in APP/PS1$^+$ mouse cortex was significantly enhanced compared to wild-type (black bar compared to grey bar; Fig. 6E and Supplementary Fig. 5A). Enhanced cortical phospho-eEF2(T56) levels were not significantly altered by removal of one allele of either *Prnp* or *Grm5* (red and purple bar compared to black bar; Fig. 6E and Supplementary Fig. 5A). Phospho-eEF2(T56) levels in APP/PS1$^+$ cortex were significantly reduced by lowering the gene dosage of both *Prnp* and *Grm5* as well as by full genetic deletion of either *Prnp* or *Grm5* (green, yellow and blue bar compared to black bar; Fig. 6E and Supplementary Fig. 5A). Thus, enhanced activation of Pyk2 and eEF2 in transgenic mouse brain is mediated by *Prnp*-*Grm5* genetic interaction, being absent in transheterozygous or full knockout transgenic brain.

We further observed reduced phosphorylation levels of CamKII at T286 in hippocampus and cortex of APP/PS1$^+$ mice compared to wild-type (black bar compared to grey bar; Fig. 6A, F and G and Supplementary Fig. 5A). Reduced phospho-CamKII(T286) levels in APP/PS1$^+$ brain were significantly enhanced by genetic deletion of *Prnp* in hippocampus (yellow bar compared to black bar; Fig. 6F and Supplementary Fig. 5A) or genetic deletion of either *Prnp* or *Grm5* in cortex (yellow and blue compared to black bar; Fig. 6A and G). The cerebellum, a brain area largely unaffected in Alzheimer's disease, did not reveal any changes in phosphorylation of Pyk2(Y402), eEF2(T56) or CamKII(T286) in APP/PS1$^+$ mice compared to wild-type littermates (Supplementary Fig. 5). Further, we did not observe changes in phosphorylation states of Pyk2(Y402), eEF2(T56) or CamKII(T286) in *Prnp*$^{-/-}$ and *Grm5*$^{-/-}$ brain in absence of the APP/PS1$^+$ transgene (Supplementary Fig. 6). Together, these phosphorylation

**Figure 6** Continued
(***$P < 0.001$; **$P < 0.01$; *$P < 0.05$). (**C**) Cortical phospho-Pyk2(Y402) levels. (**D** and **E**) eEF2(T56) phosphorylation is increased in APP/PS1$^+$ hippocampus (**D**; ****$P < 0.0001$) and cortex (**E**; *$P < 0.05$), which is not different to APP/PS1$^+$ single het erozygous brain areas. Enhanced phospho-eEF2(T56) levels are significantly reduced in APP/PS1$^+$ *Prnp*$^{+/-}$ *Grm5*$^{+/-}$, APP/PS1$^+$ *Prnp*$^{-/-}$ and APP/PS1$^+$ *Grm5*$^{-/-}$ brain areas (***$P < 0.001$; **$P < 0.01$; *$P < 0.05$). (**F** and **G**) CamKII phosphorylation at T286 is significantly reduced in APP/PS1$^+$ hippocampus (***$P < 0.001$) and cortex (*$P < 0.05$), which is not different to APP/PS1$^+$ single het erozygous brain areas. Reduced phosphorylation is enhanced by genetic deletion of *Prnp* in hippocampus and cortex or by genetic deletion of *Grm5* in cortex by one-way ANOVA with Fisher's LSD *post hoc* pairwise comparisons (*$P < 0.05$). ns = not significant.

studies provide genetic evidence that $PrP^C$ and mGluR5 cooperate in mediating altered neuronal signalling in selective Alzheimer's disease transgenic brain areas.

## Time dependence for CamKII activation after acute amyloid-β oligomer stimulation

Chronic exposure to the APP/PS1$^+$ transgene revealed alterations of Pyk2 phosphorylation at Y402 that were similar to acute amyloid-β oligomer treatment. In contrast, we observed that amyloid-β oligomer triggered enhanced CamKII phosphorylation at T286 by acute amyloid-β oligomer treatment but reduced CamKII phosphorylation at T286 after chronic exposure to the APP/PS1$^+$ transgene. To investigate differences in CamKII activation between short-term amyloid-β oligomer stimulation and chronic exposure to amyloid-β oligomers, we compared phospho-CamKII(T286) levels in acute wild-type brain slices exposed to amyloid-β oligomers for different periods of time. As amyloid-β oligomers are unstable in artificial CSF due to spontaneous fibrilization (Supplementary Fig. 7A), acute brain slices were exposed to a fresh bath of amyloid-β oligomers after every hour. We observed a significant interaction of CamKII phosphorylation at T286 between amyloid-β oligomer treatment and duration of treatment by two-way ANOVA with *post hoc* Tukey's multiple comparisons test (Supplementary Fig. 8A and B). Treatment of slices with 1 μM amyloid-β oligomers for 0.5 h triggered an initial increase in CamKII phosphorylation at T286 (Supplementary Fig. 8A and B). Phospho-CamKII(T286) levels were significantly reduced 3 h and 6 h after treatment (Supplementary Fig. 8A and B).

Activation of Pyk2 at Y402 in acute brain slices, on the other hand, was consistently enhanced by treatment with amyloid-β oligomers from 0.5–6 h (Supplementary Fig. 8A and C). We sought to recapitulate activation of eEF2 as seen in the chronic APP/PS1$^+$ Alzheimer's disease model by amyloid-β oligomer treatment of acute brain slices. Amyloid-β oligomers triggered enhanced eEF2 phosphorylation at T56 6 h after stimulation (Supplementary Fig. 8A and D).

We used immunostaining for phospho-CamKII(T286) of dissociated 21 day *in vitro* primary cortical neurons as a second approach to analyse the time-course of CamKII activation at T286 induced by amyloid-β oligomer stimulation. As amyloid-β oligomers are stable in Neurobasal® A medium at 37°C and 5% $CO_2$ (Supplementary Fig. 7B), cortical neurons were exposed to 1 μM amyloid-β oligomers and incubated for indicated times. We found a significant interaction between treatment and duration of treatment by two-way ANOVA with *post hoc* Tukey's multiple comparisons test (Supplementary Fig. 8E and F), similar to what we observed by amyloid-β oligomer stimulation of acute brain slices. Amyloid-β oligomers trigger an initial increase of phospho-CamKII(T286) intensity, which reverts to vehicle levels at 3 h of treatment and declines below vehicle levels 6 h after treatment (Supplementary Fig. 8E and F). Together, these experiments show that short-term exposure to amyloid-β oligomers activates CamKII at T286, but long-term amyloid-β oligomer treatment or chronic exposure to Alzheimer's disease transgenes deactivates CamKII at T286.

## Genetic coupling between *Prnp* and *Grm5* mediates reduced survival in Alzheimer's disease model mice

We questioned whether more complex phenotypes are also dependent on the genetic coupling between $PrP^C$ and mGluR5 in APP/PS1$^+$ Alzheimer's model mice. Mouse survival of wild-type, APP/PS1$^+$, APP/PS1$^+$ *Prnp*$^{+/-}$, APP/PS1$^+$ *Grm5*$^{+/-}$, APP/PS1$^+$ *Prnp*$^{+/-}$ *Grm5*$^{+/-}$, APP/PS1$^+$ *Prnp*$^{-/-}$ and APP/PS1$^+$ *Grm5*$^{-/-}$ mice was monitored over 600 days. After 600 days, the majority of APP/PS1$^+$ mice died, compared to only 8% of wild-type mice (black line compared to grey line; Fig. 7). Full genetic deletion of either *Prnp* or *Grm5* significantly improved mouse survival in APP/PS1$^+$ mice (blue and yellow line compared to black line; loss of 7% and 17% after 600 days; Fig. 7). Removal of one allele of either *Prnp* or *Grm5* did not benefit mouse survival (red line and purple line compared to black line; Fig. 7). Genetic removal of one allele of both *Prnp* and *Grm5* significantly improved survival of APP/PS1$^+$ mice (green line compared to black line; Fig. 7). We conclude that reduced survival of APP/PS1$^+$ mice depends on the genetic interaction of $PrP^C$ and mGluR5.

## Genetic coupling between *Prnp* and *Grm5* mediates loss of synaptic markers in Alzheimer's disease model brain *in vivo*

Synapse loss is one of the hallmarks of Alzheimer's disease that is observable in Alzheimer's disease transgenic mouse models (Scheff *et al.*, 1990; Jacobsen *et al.*, 2006). Previous studies revealed that synapse loss of APP/PS1$^+$ mice is dependent on the genetic presence of *Prnp* (Gimbel *et al.*, 2010) and can be recovered by mGluR5 antagonism (Um *et al.*, 2013). We sought to investigate whether or not synapse density in the dentate gyrus is mediated by a genetic coupling between *Prnp* and *Grm5*. Loss of synaptic markers of APP/PS1$^+$ mice (black bar compared to grey bar; Fig. 8) was fully rescued to wild-type levels by genetic deletion of *Prnp* or *Grm5* (yellow and blue bar compared to grey bar; Fig. 8). Notably, removal of one allele of either *Prnp* or *Grm5* did not benefit synapse loss in APP/PS1$^+$ brain (red and purple bar compared to black bar; Fig. 8). However, removal of one allele of both *Prnp* and *Grm5* fully rescued loss of synaptic markers to wild-type levels

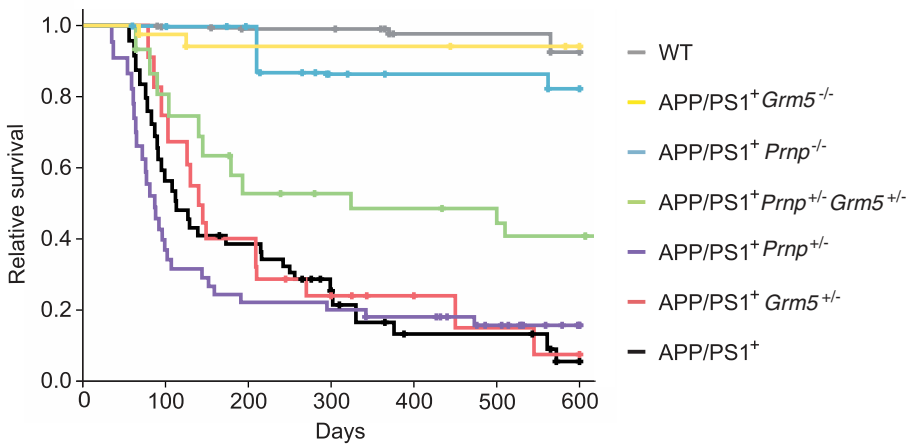


| | | | | | | | |
|---|---|---|---|---|---|---|---|
| APP/PS1$^+$ | - | + | + | + | + | + | + |
| *Prnp* | +/+ | +/+ | +/- | +/+ | +/- | -/- | +/+ |
| *Grm5* | +/+ | +/+ | +/+ | +/- | +/- | +/+ | -/- |
| Pairwise comparison to APP/PS1$^+$ *P* = | 0.001 | - | 0.591 | 0.284 | 0.032 | 0.002 | 0.009 |
| Mean survival ± SEM | 591±4 | 207±6 | 230±13 | 182±6 | 395±17 | 545±6 | 571±20 |
| *n* = | 106 | 47 | 24 | 44 | 33 | 65 | 10 |

**Figure 7 Genetic coupling between *Prnp* and *Grm5* mediates reduced survival of Alzheimer's model mice.** Survival of wild-type, APP/PS1$^+$, APP/PS1$^+$ *Prnp*$^{+/-}$, APP/PS1$^+$ *Grm5*$^{+/-}$, APP/PS1$^+$ *Prnp*$^{+/-}$ *Grm5*$^{+/-}$, APP/PS1$^+$ *Prnp*$^{-/-}$ and APP/PS1$^+$ *Grm5*$^{-/-}$ over 600 days. Survival of APP/PS1$^+$ transgenic mice is significantly shorter than of wild-type mice ($P$ = 0.001), which is recovered in APP/PS1$^+$ *Prnp*$^{+/-}$ *Grm5*$^{+/-}$ ($P$ = 0.032), APP/PS1$^+$ *Prnp*$^{-/-}$ ($P$ = 0.002), and APP/PS1$^+$ *Grm5*$^{-/-}$ mice ($P$ = 0.009) by Wilcoxon statistics with cases weighted by numbers in each group. $n$ = 106 wild-type mice, $n$ = 47 APP/PS1$^+$ mice, $n$ = 24 APP/PS1$^+$ *Prnp*$^{+/-}$ mice, $n$ = 44 APP/PS1$^+$ *Grm5*$^{+/-}$ mice, $n$ = 33 APP/PS1$^+$ *Prnp*$^{+/-}$ *Grm5*$^{+/-}$ mice, $n$ = 65 APP/PS1$^+$ *Prnp*$^{-/-}$ mice, $n$ = 10 APP/PS1$^+$ *Grm5*$^{-/-}$ mice.

(no significant difference between grey and green bar; Fig. 8). Thus, synapse loss in APP/PS1$^+$ mice is mediated through an interaction between *Prnp* and *Grm5*.

## Amyloid-β levels and enhanced gliosis are independent of the genetic presence of *Prnp* and *Grm5*

PrP$^C$ and mGluR5 are predicted to function as a complex mediating synaptic disruption in neurons downstream of amyloid-β oligomers, but not to alter amyloid-β accumulation or the responses of other cell types to amyloid-β pathology. We compared amyloid-β levels in wild-type, APP/PS1$^+$, APP/PS1$^+$ *Prnp*$^{+/-}$, APP/PS1$^+$ *Grm5*$^{+/-}$, APP/PS1$^+$ *Prnp*$^{+/-}$ *Grm5*$^{+/-}$, APP/PS1$^+$ *Prnp*$^{-/-}$ and APP/PS1$^+$ *Grm5*$^{-/-}$ brain. We observed highly enhanced amyloid-β levels by amyloid-β immunostaining as well as amyloid-β dense-core plaques by thioflavin-S staining in APP/PS1$^+$ brain compared to wild-type brain (black bar compared to grey bar; Supplementary Fig. 9A–C). We further analysed amyloid-β levels by amyloid-β ELISA and amyloid-β oligomer-dependent PrP$^C$-linked immunosorbent assay and, again, found enhanced amyloid-β levels in APP/PS1$^+$ brain (black squares compared to grey squares; Supplementary Fig. 9D and E). However, we did not find differences in amyloid-β levels within APP/PS1$^+$ groups in any of these measurements (black bars/squares compared to red, purple, green, yellow and blue bars/squares; Supplementary Fig. 9). Thus, the PrP$^C$/mGluR5 complex does not regulate amyloid-β levels.

Alzheimer's disease pathology is associated with inflammation, as marked by activated microglia and astrocytes, in areas severely affected with amyloid-β plaque deposition (Itagaki *et al.*, 1989). We analysed gliosis by immunostaining of astrocytes (GFAP) and microglia (Iba1). Our data revealed an increase in gliosis in APP/PS1$^+$ brain compared to wild-type (black bar compared to grey bar; Supplementary Fig. 10A–C). However, there was no difference within APP/PS1$^+$ groups (black bar compared to red, purple, green, yellow or blue bar; Supplementary Fig. 10A–C). Moreover, we observed enhanced expression of anti-interleukin-1 beta in the hippocampus and cortex of APP/PS1$^+$ mice compared to wild-type by immunoblot (black bar compared to grey bar; Supplementary Fig. 10D–F). Again, we did not observe any differences in

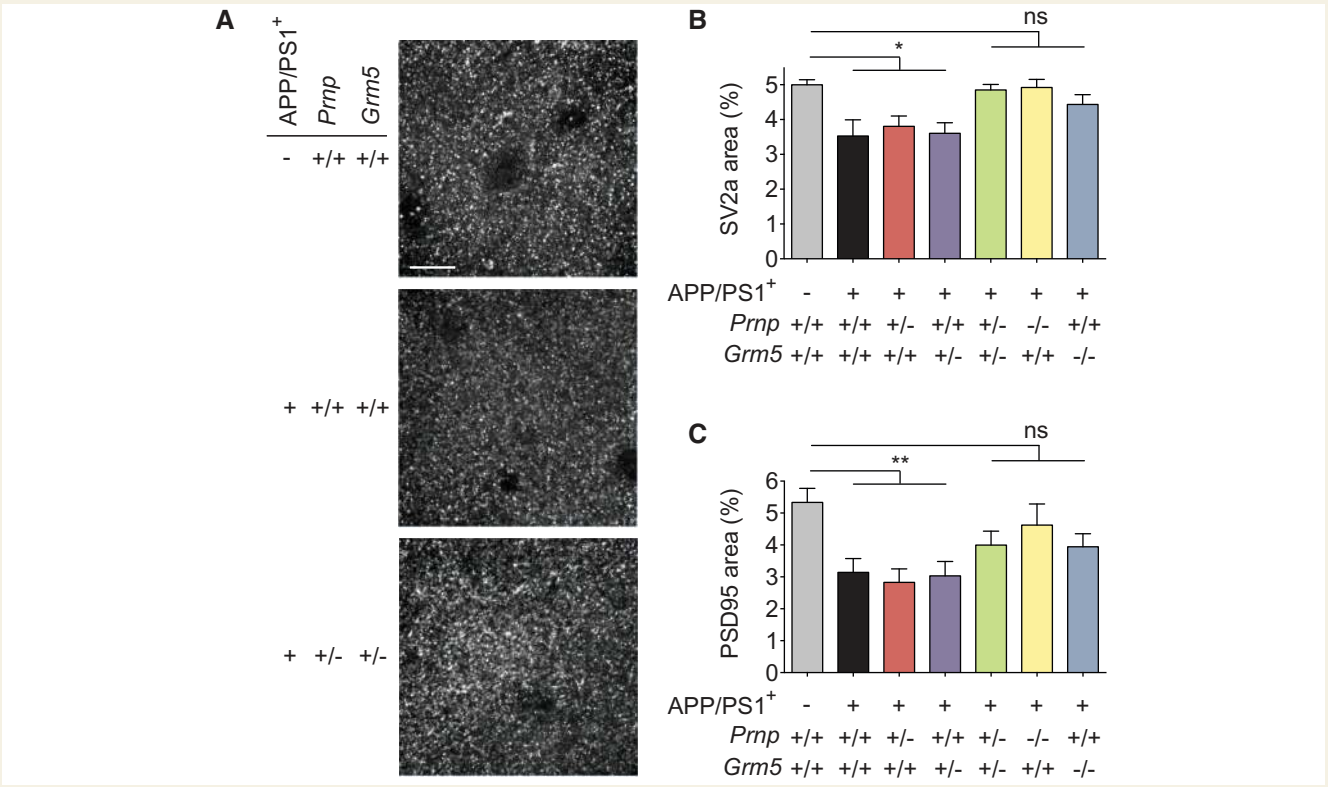


**Figure 8 Genetic coupling between *Prnp* and *Grm5* mediates loss of synaptic markers in Alzheimer's model mice *in vivo*.** (**A**) Representative confocal images of the dentate gyrus of indicated groups stained with SV2a at an average age of 666 ± 35 days. Scale bar = 12 μm. (**B** and **C**) Fractional area of immunoreactive puncta for SV2a (**B**) and PSD95 (**C**) in the dentate gyrus of the indicated groups. A one-way ANOVA with Fisher's LSD *post hoc* pairwise comparisons shows that the APP/PS1$^+$ and APP/PS1$^+$ single heterozygote groups differ from the wild-type group (*$P < 0.05$; **$P < 0.01$), but the double heterozygote and single knockout groups are not significantly different to the wild-type group ($P > 0.05$). Data are mean ± SEM, $n = 4$ mice per group, with nine images from three slices analysed per mouse. ns = not significant.

interleukin-1 beta expression within APP/PS1$^+$ groups (black bar compared to red, purple, green, yellow or blue bar; Supplementary Fig. 10D–G). Thus, *Prnp-Grm5* genetic interaction does not alter the chronic response to amyloid-β accumulation in cell types other than neurons.

# Discussion

The major finding of the current study is that PrP$^C$ and mGluR5 function as a neuronal complex to mediate amyloid-β oligomer action and Alzheimer's disease-related phenotypes. While previous studies have implicated both proteins in Alzheimer's disease pathophysiology and revealed co-immunoprecipitation between them, the genetic and biochemical data here reveal an essential role for their coupling in Alzheimer's disease-related models. Moreover, the phosphorylation state of these intracellular signalling partners of PrP$^C$ is specifically regulated by amyloid-β oligomers and Alzheimer's disease transgenes through the genetic coupling of PrP$^C$ and mGluR5, such that trans-heterozygotes, but not single heterozygotes, are rescued from amyloid-β oligomer signalling. Chronic effects on mouse survival and loss of synaptic profiles also depend upon the genetic interaction between PrP$^C$ and mGluR5.

These data may also shed light on the potential physiological role of PrP$^C$. Despite enormous advances in understanding the role of prion protein in prion disease, the function of PrP$^C$ remains elusive. Genetic deletion of *Prnp* in mice does not elicit a direct phenotype (Bueler *et al.*, 1993). Thus, understanding the endogenous function of PrP$^C$ remains a priority. This can be achieved by identifying protein partners that interact with PrP$^C$. We are the first to show that intracellular signalling partners associate with PrP$^C$ via mGluR5. Strikingly, PrP$^C$ and mGluR5 function as a neuronal complex to mediate amyloid-β oligomer pathophysiology in mouse and human brain. Despite this role in the disease state, glutamate-dependent signalling is not altered by the presence of PrP$^C$ under normal physiological conditions (Um *et al.*, 2013). It is possible that unidentified physiological PrP$^C$ partners control mGluR5 function in a manner usurped by pathological amyloid-β oligomers in Alzheimer's disease. The current findings suggest that mGluR5-dependent assays may serve as a tool to understand physiological PrP$^C$ functions.

## mGluR5 couples PrP$^C$ to intracellular protein mediators

We report that PrP$^C$ is linked by mGluR5 to the intracellular protein mediators Homer1b/c, Pyk2 and CamKII via mGluR5. Co-immunoprecipitation between PrP$^C$ and intracellular proteins requires co-expression of either Myc-mGluR5 or Myc-mGluR1 in HEK-293T cells. In acute brain slice crude synaptoneurosome fractions, co-immunoprecipitation is essentially eliminated by genetic deletion of *Grm5*. This indicates that GPI (glycosyl-phosphatidyl-inositol)-anchored PrP$^C$ coupling to the here-analysed protein mediators within the cell requires mGluR5, or mGluR1. We further show that amyloid-β oligomers modulated the coupling between PrP$^C$ and intracellular protein mediators in HEK-293T cells and acute mouse brain slices. Notably, amyloid-β oligomers were only capable of altering the interaction between mGluR5 and intracellular protein mediators in HEK-293T cells and primary hippocampal neurons in the presence of PrP$^C$. These results provide further evidence for PrP$^C$ as a functional cell-surface receptor site of amyloid-β oligomers. Interestingly, we found a pathologically reduced association between PrP$^C$ and Pyk2 as well as between PrP$^C$ and Homer1b/c both in Alzheimer's disease mouse model brain and human post-mortem Alzheimer's disease brain compared to age-matched controls. Similarly, a pathologically reduced association between mGluRs and Homer has been demonstrated in several neurological diseases, including fragile X syndrome and Angelman syndrome (Giuffrida *et al.*, 2005; Pignatelli *et al.*, 2014). This pathological situation is predicted to prevent physiologically fluctuating levels of glutamate to regulate the interaction between mGluR5 and intracellular signalling proteins.

The simplest model for amyloid-β oligomer signalling is that Alzheimer's disease-derived oligomers induce a conformational change in their PrP$^C$ binding site, which is transmitted via protein-protein interaction to mGluR5, and subsequently to its intracellular mediators. In addition, higher order mGluR5 protein assembly states and lateral mobility might contribute to signal transduction. It has been demonstrated that amyloid-β oligomers trigger clustering of mGluR5 in primary hippocampal neurons under conditions in which anti-PrP$^C$ antibodies reduce neuronal binding (Renner *et al.*, 2010). Under physiological conditions, the stabilization of synaptic proteins within the plasma membrane is transient, with constant lateral movement of receptors such as mGluR5 (Triller and Choquet, 2008). The presence of the amyloid-β oligomer ligand appears to generate a pathophysiological state where mGluR5 is scaffolded by the stabilized amyloid-β oligomer-PrP$^C$ complex. Prevention of the lateral movement of mGluR5 within the plasma membrane is likely to alter changes within the mGluR5 multiprotein complex that normally occur in response to glutamate stimulation. For example, amyloid-β oligomer-induced overstabilization of mGluR5 may alter intracellular $Ca^{2+}$ levels (Renner *et al.*, 2010). Both conformational changes within the mGluR5 multiprotein complex and altered $Ca^{2+}$ levels may drive the amyloid-β oligomer-induced acute activation of Pyk2 and CamKII observed here.

PrP$^C$ interaction with mGluR5 has been observed in several situations in addition to our previous analysis of PrP$^C$ coupling to FYN kinase (Um *et al.*, 2013). Amyloid-β oligomer-induced long-term depression (LTD) is dependent on both mGluR5 and PrP$^C$ (Hu *et al.*, 2014). Also, amyloid-β oligomer-induced redistribution of CamKIIα into cytoplasmic puncta is dependent on the co-expression of mGluR5 with PrP$^C$ (Raka *et al.*, 2015). Furthermore, studies of laminin signalling after PrP$^C$ binding demonstrate mGluR5 mediated increases of intracellular $Ca^{2+}$ levels (Beraldo *et al.*, 2011). Thus, mGluR5 seems to transduce different signals from PrP$^C$ onto intracellular signalling mediators.

## Association between mGluR5 and intracellular protein mediators

In the current study, PrP$^C$ is associated via mGluR5 with Homer1b/c, Pyk2 and CamKII. Previous work confirmed a physical interaction between the postsynaptic scaffolding protein Homer and the C-terminal proline-rich sequence of mGluRs (Brakeman *et al.*, 1997). It has been shown that stimulation by agonist quisqualate enhances co-immunoprecipitation between Homer and class I mGluRs, whereas mGluR antagonism by MPEP reduces association (Rong *et al.*, 2003). Amyloid-β treatment of cortical neurons is reported to decrease synaptic levels of Homer1b (Roselli *et al.*, 2009). Here we show that amyloid-β oligomer treatment triggers dissociation of Homer1b/c from the PrP$^C$-mGluR5 complex. Further, chronic exposure to amyloid-β oligomers in humans or mice causes a pathological state, where Homer1b/c is less associated with the PrP$^C$-mGluR5 complex. We hypothesize that in this state, glutamate-dependent activation of the receptor is less capable of stimulating physiological changes in Homer1b/c. It has been shown previously that disruption of the interaction between mGluR5 and Homer prevents mGluR-LTD as well as mGluR-induced signalling cascades (Ronesi and Huber, 2008). Thus, the pathological effect of amyloid-β oligomers could be due to blocking signalling events that depend on association changes between mGluR5 and intracellular mediators like Homer1b/c.

Other studies reported the association between CamKII and the intracellular C-terminal tail as well as the intracellular loop 2 of mGluR5 (Jin *et al.*, 2013*a*, *b*; Raka *et al.*, 2015). $Ca^{2+}$ stimulation triggers dissociation of CamKIIα from mGluR5 in rat striatal neurons, which is hypothesized to facilitate LTP induction (Jin *et al.*, 2013*b*). In contrast, amyloid-β oligomer treatment triggers enhanced association between CamKIIα and mGluR5 (Raka *et al.*, 2015). Thus, the potent inhibition of LTP by amyloid-β oligomers may depend in part on CamKII being unable to dissociate from

mGluR5 in the presence of amyloid-β oligomers. Our data further revealed acute short-term amyloid-β oligomer treatment to phosphorylate CamKII at T286, but chronic exposure to the APP/PS1$^+$ transgene to dephosphorylate CamKII at T286. To address this difference, we analysed phospho-CamKII(T286) levels after varying times of amyloid-β oligomer treatment in acute brain slices and primary cortical cultures. We found that phospho-CamKII(T286) levels were initially increased by amyloid-β oligomers, returned to basal levels at 3 h of treatment and slightly declined below basal at 6 h of amyloid-β oligomer treatment. Similar to what we observed with acute amyloid-β oligomer treatment, glutamate stimulation of cortical neurons induces rapid phosphorylation of CamKII, which returns to basal levels 1.5 h after washout of glutamate, followed by a slight decline below basal levels 2.5 h after washout (Hosokawa *et al.*, 2006). Under physiological conditions, activated phospho(T286)-CamKII dissociates from the mGluR5 complex. Phospho(T286)-CamKII then associates with and phosphorylates NMDAR GluN2B subunits (Jin *et al.*, 2013*b*). We hypothesize that this physiological event is unable to occur in the presence of excess amyloid-β oligomers, which affects synaptic plasticity.

Further studies showed association between mGluR5 and Pyk2 in rat brain as well as co-localization of mGluR5 and Pyk2 in cortical neurons (Nicodemo *et al.*, 2010). Pyk2 is known to dissociate from mGluR1 after treatment with quisqualate in HEK-293T cells (Nicodemo *et al.*, 2010), similar to what we observed in HEK-293T cells and acute mouse brain slices after amyloid-β oligomer treatment.

## Genetic coupling between *Prnp* and *Grm5* alters protein activation, plasticity, synaptic density and survival

We found that the genetic interaction between *Prnp* and *Grm5* is significantly involved in mediating amyloid-β oligomer-induced phosphorylation of intracellular proteins and inhibition of LTP acutely. Our data further confirmed a genetic coupling between *Prnp* and *Grm5* in mediating alterations in protein activation states selectively in APP/PS1$^+$ transgenic hippocampus and cortex. Notably, a selective vulnerability for brain areas such as neocortex and hippocampus towards Alzheimer's disease pathogenesis exists (Morrison and Hof, 1997). Our results show that intracellular protein mediators are selectively altered in hippocampus and cortex of Alzheimer's disease transgenic model mice compared to wild-type. All members of the here-studied signalling cascade are present in the cerebellum. Yet, no activation changes of intracellular protein mediators were observed in transgenic cerebellum compared to wild-type. We speculate that regional differences in the interaction between proteins of the here-studied signalling pathway contribute to differences in amyloid-β oligomer-dependent protein activation states. This regional vulnerability to amyloid-β oligomers might make hippocampal and cortical neurons more prone to degeneration compared to cerebellar neurons during Alzheimer's disease progression.

Our previous work and other studies demonstrated amyloid-β oligomer/PrP$^C$-mediated activation of the non-receptor tyrosine kinase FYN (Larson *et al.*, 2012; Um *et al.*, 2012). Furthermore, mGluR5 is implicated in this pathway (Um *et al.*, 2013). FYN phosphorylation of NR2A and NR2B subunits alters trafficking of NMDA receptors, which regulates synaptic plasticity (Grant *et al.*, 1992; Suzuki and Okumura-Noji, 1995; Nakazawa *et al.*, 2001). Critically, amyloid-β oligomer binding to PrP$^C$ also triggers tau phosphorylation (Larson *et al.*, 2012). Evidence exists for a genetic interaction between FYN and tau to regulate synapse density and behaviour in APP transgenic mice (Chin *et al.*, 2004, 2005; Roberson *et al.*, 2011). Notably, amyloid-β oligomer-induced phosphorylation of eEF2 in cortical neurons is dependent on FYN signalling and the kinase inhibitor sarcatinib fully blocks amyloid-β oligomer-induced eEF2 phosphorylation (Um *et al.*, 2013). The data indicate that the amyloid-β oligomer/PrP$^C$/mGluR5 complex activates different signalling pathways, some of which are dependent on FYN kinase activation. Moreover, eEF2 signalling occurs downstream of FYN signalling and is dependent on the genetic presence of *Prnp* and *Grm5* (Um *et al.*, 2013). Based on the findings of this manuscript, we hypothesize that FYN activation is also dependent on the genetic interaction between *Prnp* and *Grm5*. It is important to note that acute activation of FYN via amyloid-β oligomer/PrP$^C$/mGluR5 leads to compensatory changes including increased STEP phosphatase (*PTPN5*), that return phospho-FYN levels to baseline (Um *et al.*, 2012), and prevent assessment of FYN during chronic activation *in vivo*. The relative roles and interplay of FYN, eEF2, Pyk2, CamKII and calcium levels as mediators of the pathophysiological amyloid-β oligomer/PrP$^C$/mGluR5 complex will require future studies.

Critically, we also found that amyloid-β oligomer-PrP$^C$ coupling to mGluR5 is responsible for reduced survival and synapse loss in APP/PS1$^+$ mice compared to wild-type. Notably, these phenotypes are recovered without altered gliosis, β-amyloid plaque load or amyloid-β oligomer levels. This suggests that the recovery in APP/PS1$^+$ *Prnp*$^{+/-}$ *Grm5*$^{+/-}$ mice is fully dependent on targeting amyloid-β oligomer-induced alterations in neuronal signalling pathways related to Alzheimer's disease in these mice. Genetic removal of *Prnp* or *Grm5*, as well as the double heterozygote state, is sufficient to rescue disease progression in APP/PS1$^+$ mice without altered amyloid-β accumulation or gliosis. Improvements occur in response to removal of the amyloid-β oligomer cell-surface anchor PrP$^C$ (Lauren *et al.*, 2009; Gimbel *et al.*, 2010), the transmembrane signal transducer mGluR5 (Um *et al.*, 2013), or a reduced interaction between both proteins in the current study.

## Targeting the $PrP^C$-mGluR5 interaction for Alzheimer's disease therapy

The current work verified a significant interaction between *Prnp* and *Grm5* in mediating amyloid-β oligomer-induced phenotypes and provides further evidence for the amyloid-β oligomer-$PrP^C$-mGluR5 pathway in Alzheimer's disease pathophysiology. The data show that improvements of Alzheimer's disease-like phenotypes in APP/PS1$^+$ mice occurred despite continued high levels of amyloid-β, amyloid-β oligomers, and amyloid-β plaques. We hypothesize that targeting the $PrP^C$-mGluR5 interaction in Alzheimer's disease will ameliorate disease progression by reducing the signal transduction from extracellular amyloid-β oligomers onto intracellular protein mediators, a mechanism distinct from amyloid-β lowering agents. We have shown previously that $PrP^C$-directed antibodies and mGluR5-directed compounds can potently modulate the interaction between $PrP^C$ and mGluR5 (Haas *et al.*, 2014). Additional studies will further clarify the efficacy of these molecules to ameliorate Alzheimer's disease phenotypes without negatively affecting endogenous signalling.

# Acknowledgements

We thank Jacqueline Heiss and Stefano Sodi for assistance with mouse husbandry.

# Funding

This work was supported by grants from NIH, BrightFocus Foundation, Alzheimer's Association and Falk Medical Research Trust to S.M.S., and the German National Academic Foundation supports L.T.H.

# Disclosure

S.M.S. is a co-founder of Axerion Therapeutics seeking to develop PrP-based therapeutics for Alzheimer disease.

# Supplementary material

Supplementary material is available at *Brain* online.

# References

Amada N, Aihara K, Ravid R, Horie M. Reduction of NR1 and phosphorylated Ca2+/calmodulin-dependent protein kinase II levels in Alzheimer's disease. Neuroreport 2005; 16: 1809–13.

Ango F, Prezeau L, Muller T, Tu JC, Xiao B, Worley PF, et al. Agonist-independent activation of metabotropic glutamate receptors by the intracellular protein Homer. Nature 2001; 411: 962–5.

Balducci C, Beeg M, Stravalaci M, Bastone A, Sclip A, Biasini E, et al. Synthetic amyloid-beta oligomers impair long-term memory independently of cellular prion protein. Proc Natl Acad Sci USA 2010; 107: 2295–300.

Barry AE, Klyubin I, Mc Donald JM, Mably AJ, Farrell MA, Scott M, et al. Alzheimer's disease brain-derived amyloid-beta-mediated inhibition of LTP in vivo is prevented by immunotargeting cellular prion protein. J Neurosci 2011; 31: 7259–63.

Bate C, Williams A. Amyloid-beta-induced synapse damage is mediated via cross-linkage of cellular prion proteins. J Biol Chem 2011; 286: 37955–63.

Bear MF, Huber KM, Warren ST. The mGluR theory of fragile X mental retardation. Trends Neurosci 2004; 27: 370–7.

Beraldo FH, Arantes CP, Santos TG, Machado CF, Roffe M, Hajj GN, et al. Metabotropic glutamate receptors transduce signals for neurite outgrowth after binding of the prion protein to laminin gamma1 chain. FASEB J 2011; 25: 265–79.

Brakeman PR, Lanahan AA, O'Brien R, Roche K, Barnes CA, Huganir RL, et al. Homer: a protein that selectively binds metabotropic glutamate receptors. Nature 1997; 386: 284–8.

Bueler H, Aguzzi A, Sailer A, Greiner RA, Autenried P, Aguet M, et al. Mice devoid of PrP are resistant to scrapie. Cell 1993; 73: 1339–47.

Calella AM, Farinelli M, Nuvolone M, Mirante O, Moos R, Falsig J, et al. Prion protein and Abeta-related synaptic toxicity impairment. EMBO Mol Med 2010; 2: 306–14.

Chen S, Yadav SP, Surewicz WK. Interaction between human prion protein and amyloid-beta (Abeta) oligomers: role OF N-terminal residues. J Biol Chem 2010; 285: 26377–83.

Chin J, Palop JJ, Puolivali J, Massaro C, Bien-Ly N, Gerstein H, et al. Fyn kinase induces synaptic and cognitive impairments in a transgenic mouse model of Alzheimer's disease. J Neurosci 2005; 25: 9694–703.

Chin J, Palop JJ, Yu GQ, Kojima N, Masliah E, Mucke L. Fyn kinase modulates synaptotoxicity, but not aberrant sprouting, in human amyloid precursor protein transgenic mice. J Neurosci 2004; 24: 4692–7.

Chung E, Ji Y, Sun Y, Kascsak RJ, Kascsak RB, Mehta PD, et al. Anti-PrPC monoclonal antibody infusion as a novel treatment for cognitive deficits in an Alzheimer's disease model mouse. BMC Neurosci 2010; 11: 130.

Dohler F, Sepulveda-Falla D, Krasemann S, Altmeppen H, Schluter H, Hildebrand D, et al. High molecular mass assemblies of amyloid-beta oligomers bind prion protein in patients with Alzheimer's disease. Brain 2014; 137(Pt 3): 873–86.

Fluharty BR, Biasini E, Stravalaci M, Sclip A, Diomede L, Balducci C, et al. An N-terminal fragment of the prion protein binds to amyloid-beta oligomers and inhibits their neurotoxicity in vivo. J Biol Chem 2013; 288: 7857–66.

Freir DB, Nicoll AJ, Klyubin I, Panico S, Mc Donald JM, Risse E, et al. Interaction between prion protein and toxic amyloid beta assemblies can be therapeutically targeted at multiple sites. Nat Commun 2011; 2: 336.

Gimbel DA, Nygaard HB, Coffey EE, Gunther EC, Lauren J, Gimbel ZA, et al. Memory impairment in transgenic Alzheimer mice requires cellular prion protein. J Neurosc 2010; 30: 6367–74.

Giuffrida R, Musumeci S, D'Antoni S, Bonaccorso CM, Giuffrida-Stella AM, Oostra BA, et al. A reduced number of metabotropic glutamate subtype 5 receptors are associated with constitutive homer proteins in a mouse model of fragile X syndrome. J Neurosci 2005; 25: 8908–16.

Grant SG, O'Dell TJ, Karl KA, Stein PL, Soriano P, Kandel ER. Impaired long-term potentiation, spatial learning, and hippocampal development in fyn mutant mice. Science 1992; 258: 1903–10.

Haas LT, Kostylev MA, Strittmatter SM. Therapeutic molecules and endogenous ligands regulate the interaction between brain cellular prion protein (PrPC) and metabotropic glutamate receptor 5 (mGluR5). J Biol Chem 2014; 289: 28460–77.

Hamilton A, Esseltine JL, DeVries RA, Cregan SP, Ferguson SS. Metabotropic glutamate receptor 5 knockout reduces cognitive impairment and pathogenesis in a mouse model of Alzheimer's disease. Mol Brain 2014; 7: 40.

Hosokawa T, Saito T, Asada A, Ohshima T, Itakura M, Takahashi M, et al. Enhanced activation of Ca2 + /calmodulin-dependent protein kinase II upon downregulation of cyclin-dependent kinase 5-p35. J Neurosci Res 2006; 84: 747–54.

Hu NW, Nicoll AJ, Zhang D, Mably AJ, O'Malley T, Purro SA, et al. mGlu5 receptors and cellular prion protein mediate amyloid-beta-facilitated synaptic long-term depression in vivo. Nat Commun 2014; 5: 3374.

Itagaki S, McGeer PL, Akiyama H, Zhu S, Selkoe D. Relationship of microglia and astrocytes to amyloid deposits of Alzheimer disease. J Neuroimmunol 1989; 24: 173–82.

Jankowsky JL, Xu G, Fromholt D, Gonzales V, Borchelt DR. Environmental enrichment exacerbates amyloid plaque formation in a transgenic mouse model of Alzheimer disease. J Neuropathol Exp Neurol 2003; 62: 1220–7.

Jacobsen JS, Wu CC, Redwine JM, Comery TA, Arias R, Bowlby M, et al. Early-onset behavioral and synaptic deficits in a mouse model of Alzheimer's disease. Proc Natl Acad Sci USA 2006; 103: 5161–6.

Jin DZ, Guo ML, Xue B, Fibuch EE, Choe ES, Mao LM, et al. Phosphorylation and feedback regulation of metabotropic glutamate receptor 1 by calcium/calmodulin-dependent protein kinase II. J Neurosci 2013a; 33: 3402–12.

Jin DZ, Guo ML, Xue B, Mao LM, Wang JQ. Differential regulation of CaMKIIalpha interactions with mGluR5 and NMDA receptors by Ca(2 + ) in neurons. J Neurochem 2013b; 127: 620–31.

Jin M, Shepardson N, Yang T, Chen G, Walsh D, Selkoe DJ. Soluble amyloid beta-protein dimers isolated from Alzheimer cortex directly induce Tau hyperphosphorylation and neuritic degeneration. Proc Natl Acad Sci USA 2011; 108: 5819–24.

Kaufman AC, Salazar SV, Haas LT, Yang J, Kostylev MA, Jeng AT, et al. Fyn inhibition rescues established memory and synapse loss in Alzheimer mice. Ann Neurol 2015; 77: 953–71.

Kayed R, Head E, Thompson JL, McIntire TM, Milton SC, Cotman CW, et al. Common structure of soluble amyloid oligomers implies common mechanism of pathogenesis. Science 2003; 300: 486–9.

Kessels HW, Nguyen LN, Nabavi S, Malinow R. The prion protein as a receptor for amyloid-beta. Nature 2010; 466: E3–4; discussion E5.

Kiyota T, Yamamoto M, Xiong H, Lambert MP, Klein WL, Gendelman HE, et al. CCL2 accelerates microglia-mediated Abeta oligomer formation and progression of neurocognitive dysfunction. PloS One 2009; 4: e6197.

Klyubin I, Nicoll AJ, Khalili-Shirazi A, Farmer M, Canning S, Mably A, et al. Peripheral administration of a humanized anti-PrP antibody blocks Alzheimer's disease Abeta synaptotoxicity. J Neurosci 2014; 34: 6140–5.

Kostylev MA, Kaufman AC, Nygaard HB, Patel P, Haas LT, Gunther EC, et al. Prion-Protein-Interacting Amyloid-beta Oligomers of High Molecular Weight are Tightly Correlated with Memory Impairment in Multiple Alzheimer Mouse Models. J Biol Chem 2015; 290: 17415–38.

Kudo W, Lee HP, Zou WQ, Wang X, Perry G, Zhu X, et al. Cellular prion protein is essential for oligomeric amyloid-beta-induced neuronal cell death. Hum Mol Genet 2012; 21: 1138–44.

Kudo W, Petersen RB, Lee HG. Cellular prion protein and Alzheimer disease: link to oligomeric amyloid-beta and neuronal cell death. Prion 2013; 7: 114–16.

Lambert JC, Ibrahim-Verbaas CA, Harold D, Naj AC, Sims R, Bellenguez C, et al. Meta-analysis of 74,046 individuals identifies 11 new susceptibility loci for Alzheimer's disease. Nat Genet 2013; 45: 1452–8.

Lambert MP, Barlow AK, Chromy BA, Edwards C, Freed R, Liosatos M, et al. Diffusible, nonfibrillar ligands derived from Abeta1–42 are potent central nervous system neurotoxins. Proc Natl Acad Sci USA 1998; 95: 6448–53.

Larson M, Sherman MA, Amar F, Nuvolone M, Schneider JA, Bennett DA, et al. The complex PrP(c)-Fyn couples human oligomeric Abeta with pathological tau changes in Alzheimer's disease. J Neurosci 2012; 32: 16857–71a.

Lauren J, Gimbel DA, Nygaard HB, Gilbert JW, Strittmatter SM. Cellular prion protein mediates impairment of synaptic plasticity by amyloid-beta oligomers. Nature 2009; 457: 1128–32.

Lesne S, Koh MT, Kotilinek L, Kayed R, Glabe CG, Yang A, et al. A specific amyloid-beta protein assembly in the brain impairs memory. Nature 2006; 440: 352–7.

Lu YM, Jia Z, Janus C, Henderson JT, Gerlai R, Wojtowicz JM, et al. Mice lacking metabotropic glutamate receptor 5 show impaired learning and reduced CA1 long-term potentiation (LTP) but normal CA3 LTP. J Neurosci 1997; 17: 5196–205.

Ma T, Chen Y, Vingtdeux V, Zhao H, Viollet B, Marambaud P, et al. Inhibition of AMP-activated protein kinase signaling alleviates impairments in hippocampal synaptic plasticity induced by amyloid beta. J Neurosci 2014; 34: 12230–8.

Mao L, Yang L, Tang Q, Samdani S, Zhang G, Wang JQ. The scaffold protein Homer1b/c links metabotropic glutamate receptor 5 to extracellular signal-regulated protein kinase cascades in neurons. J Neurosci 2005; 25: 2741–52.

Morrison JH, Hof PR. Life and death of neurons in the aging brain. Science 1997; 278: 412–19.

Nairn AC, Palfrey HC. Identification of the major Mr 100 000 substrate for calmodulin-dependent protein kinase III in mammalian cells as elongation factor-2. J Biol Chem 1987; 262: 17299–303.

Nakazawa T, Komai S, Tezuka T, Hisatsune C, Umemori H, Semba K, et al. Characterization of Fyn-mediated tyrosine phosphorylation sites on GluR epsilon 2 (NR2B) subunit of the N-methyl-D-aspartate receptor. J Biol Chem 2001; 276: 693–9.

Nicodemo AA, Pampillo M, Ferreira LT, Dale LB, Cregan T, Ribeiro FM, et al. Pyk2 uncouples metabotropic glutamate receptor G protein signaling but facilitates ERK1/2 activation. Mol Brain 2010; 3: 4.

Nicoll AJ, Panico S, Freir DB, Wright D, Terry C, Risse E, et al. Amyloid-beta nanotubes are associated with prion protein-dependent synaptotoxicity. Nat Commun 2013; 4: 2416.

Nygaard HB, van Dyck CH, Strittmatter SM. Fyn kinase inhibition as a novel therapy for Alzheimer's disease. Alzheimers Res Ther 2014; 6: 8.

Nygaard HB, Wagner AF, Bowen GS, Good SP, MacAvoy MG, Strittmatter KA, et al. A phase Ib multiple ascending dose study of the safety, tolerability, and central nervous system availability of AZD0530 (saracatinib) in Alzheimer's disease. Alzheimers Res Ther 2015; 7: 35.

Ostapchenko VG, Beraldo FH, Mohammad AH, Xie YF, Hirata PH, Magalhaes AC, et al. The prion protein ligand, stress-inducible phosphoprotein 1, regulates amyloid-beta oligomer toxicity. J Neurosci 2013; 33: 16552–64.

Park S, Park JM, Kim S, Kim JA, Shepherd JD, Smith-Hicks CL, et al. Elongation factor 2 and fragile X mental retardation protein control the dynamic translation of Arc/Arg3.1 essential for mGluR-LTD. Neuron 2008; 59: 70–83.

Pignatelli M, Piccinin S, Molinaro G, Di Menna L, Riozzi B, Cannella M, et al. Changes in mGlu5 receptor-dependent synaptic plasticity and coupling to homer proteins in the hippocampus of Ube3A hemizygous mice modeling angelman syndrome. J Neurosci 2014; 34: 4558–66.

Raka F, Di Sebastiano AR, Kulhawy SC, Ribeiro FM, Godin CM, Caetano FA, et al. Ca(2 + )/Calmodulin-dependent protein Kinase II interacts with group I Metabotropic Glutamate and facilitates Receptor Endocytosis and ERK1/2 signaling: role of beta-Amyloid. Mol Brain 2015; 8: 21.

Reed MN, Hofmeister JJ, Jungbauer L, Welzel AT, Yu C, Sherman MA, et al. Cognitive effects of cell-derived and synthetically derived Abeta oligomers. Neurobiol Aging 2011; 32: 1784–94.

Renner M, Lacor PN, Velasco PT, Xu J, Contractor A, Klein WL, et al. Deleterious effects of amyloid beta oligomers acting as an extracellular scaffold for mGluR5. Neuron 2010; 66: 739–54.

Resenberger UK, Harmeier A, Woerner AC, Goodman JL, Muller V, Krishnan R, et al. The cellular prion protein mediates neurotoxic

signalling of beta-sheet-rich conformers independent of prion replication. EMBO J 2011; 30: 2057–70.
Roberson ED, Halabisky B, Yoo JW, Yao J, Chin J, Yan F, et al. Amyloid-beta/Fyn-induced synaptic, network, and cognitive impairments depend on tau levels in multiple mouse models of Alzheimer's disease. J Neurosci 2011; 31: 700–11.
Ronesi JA, Huber KM. Homer interactions are necessary for metabotropic glutamate receptor-induced long-term depression and translational activation. J Neurosci 2008; 28: 543–7.
Rong R, Ahn JY, Huang H, Nagata E, Kalman D, Kapp JA, et al. PI3 kinase enhancer-Homer complex couples mGluRI to PI3 kinase, preventing neuronal apoptosis. Nat Neurosci 2003; 6: 1153–61.
Roselli F, Hutzler P, Wegerich Y, Livrea P, Almeida OF. Disassembly of shank and homer synaptic clusters is driven by soluble beta-amyloid(1–40) through divergent NMDAR-dependent signalling pathways. PloS One 2009; 4: e6011.
Rushworth JV, Griffiths HH, Watt NT, Hooper NM. Prion protein-mediated toxicity of amyloid-β oligomers requires lipid rafts and the transmembrane LRP1. J Biol Chem 2013; 288: 8935–51.
Scheetz AJ, Nairn AC, Constantine-Paton M. NMDA receptor-mediated control of protein synthesis at developing synapses. Nat Neurosci 2000; 3: 211–16.
Scheff SW, DeKosky ST, Price DA. Quantitative assessment of cortical synaptic density in Alzheimer's disease. Neurobiol Aging 1990; 11: 29–37.
Shankar GM, Li S, Mehta TH, Garcia-Munoz A, Shepardson NE, Smith I, et al. Amyloid-beta protein dimers isolated directly from Alzheimer's brains impair synaptic plasticity and memory. Nat Med 2008; 14: 837–42.
Suzuki T, Okumura-Noji K. NMDA receptor subunits epsilon 1 (NR2A) and epsilon 2 (NR2B) are substrates for Fyn in the post-synaptic density fraction isolated from the rat brain. Biochem Biophys Res Commun 1995; 216: 582–8.
Triller A, Choquet D. New concepts in synaptic biology derived from single-molecule imaging. Neuron 2008; 59: 359–74.
Um JW, Kaufman AC, Kostylev M, Heiss JK, Stagi M, Takahashi H, et al. Metabotropic glutamate receptor 5 is a coreceptor for Alzheimer abeta oligomer bound to cellular prion protein. Neuron 2013; 79: 887–902.
Um JW, Nygaard HB, Heiss JK, Kostylev MA, Stagi M, Vortmeyer A, et al. Alzheimer amyloid-beta oligomer bound to postsynaptic prion protein activates Fyn to impair neurons. Nat Neurosci 2012; 15: 1227–35.
Walsh KP, Minamide LS, Kane SJ, Shaw AE, Brown DR, Pulford B, et al. Amyloid-beta and proinflammatory cytokines utilize a prion protein-dependent pathway to activate NADPH oxidase and induce cofilin-actin rods in hippocampal neurons. PloS One 2014; 9: e95995.
Wang X, Lopez OL, Sweet RA, Becker JT, DeKosky ST, Barmada MM, et al. Genetic determinants of disease progression in Alzheimer's disease. J Alzheimers Dis 2015; 43: 649–55.
Xiao B, Tu JC, Petralia RS, Yuan JP, Doan A, Breder CD, et al. Homer regulates the association of group 1 metabotropic glutamate receptors with multivalent complexes of homer-related, synaptic proteins. Neuron 1998; 21: 707–16.
Zou WQ, Xiao X, Yuan J, Puoti G, Fujioka H, Wang X, et al. Amyloid-beta42 interacts mainly with insoluble prion protein in the Alzheimer brain. J Biol Chem 2011; 286: 15095–105.